

1 **Trends in soil mercury stock associated with pollution sources on a**
2 **Mediterranean island (Majorca, Spain)**

3

4 Authors: José Antonio Rodríguez Martín ^{(1)*}, Carmen Gutiérrez ⁽²⁾, Miguel Escuer ⁽²⁾,
5 Marina Martín-Dacal ⁽³⁾, José Joaquín Ramos-Miras ⁽⁴⁾, Luis Roca-Perez ⁽⁵⁾, Rafael
6 Boluda ⁽⁵⁾, Nikos Nanos ⁽⁶⁾.

7

8 ¹ Department of Environment, Instituto Nacional de Investigación y Tecnología Agraria y
9 Alimentaria (INIA), ES-28040, Madrid, Spain. (e-mail: rmartin@inia.es)

10 ² Instituto de Ciencias Agrarias, ICA- CSIC. Serrano, 114bis. 28006 Madrid, Spain. (e-mail:
11 carmen.g@ica.csic.es)

12 ³ Centro de Biotecnología y Genómica de Plantas (UPM-INIA). Parque Científico y Tecnológico,
13 UPM Campus de Montegancedo, 28223 Madrid, Spain (e-mail: marina.md96@gmail.com)
14 marina.martind@upm.es

15 ⁴ Dpto. Didáctica Ciencias Sociales y Experimentales, Universidad de Córdoba, Avda. San
16 Alberto Magno s/n, Córdoba 14071, Spain. (e-mail: jjramos@uco.es)

17 ⁵ Dept. Biologia Vegetal, Facultat de Farmàcia, Universitat de València, Av. Vicent Andrés i
18 Estellés s/n, 46100 Burjassot, (Valencia), Spain (e-mail: boluda@uv.es)

19 ⁶ School of Forestry and Natural Environment, Aristotle University of Thessaloniki. 59
20 Moschounti str., 55134 Foinikas-Thessaloniki, Greece. (e-mail: nikosnanos@for.auth.gr)

21

22

23 *Corresponding author: e-mail: rmartin@inia.es

24 Telephone/fax number: -34 913476795/ +34 913474008

25

26

27

28

29

30

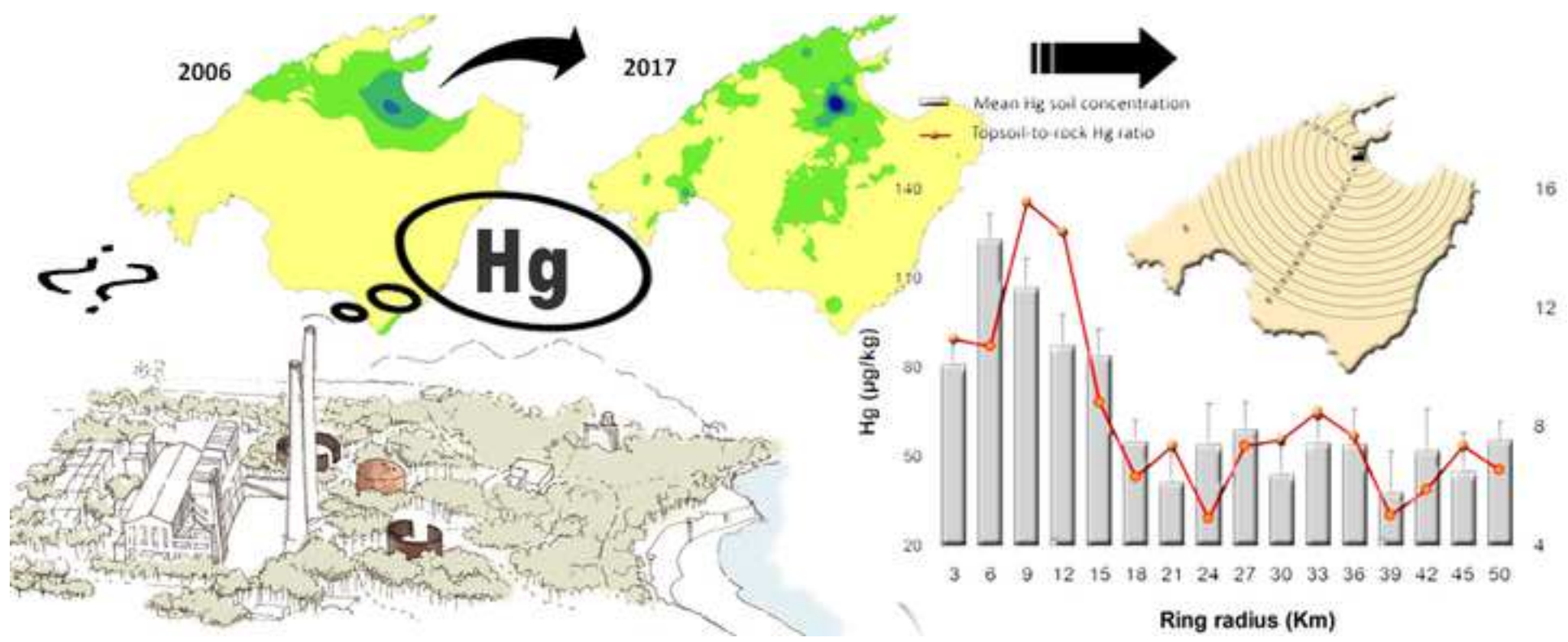
31

32

33

34

35



36 **Abstract**

37 Hg is a global concern given its adverse effects on human health, food security and the
38 environment, and it requiring actions to identify major local Hg sources and to
39 evaluate pollution. Our study provides the first assessment of Hg stock trends on the
40 entire Majorca surface, identifying major Hg sources by studying the spatiotemporal
41 soil Hg variation at two successive times (2006 and 2016-17). The Hg soil concentration
42 ranged from 14 to 258 $\mu\text{g kg}^{-1}$ (mean 52.40 $\mu\text{g kg}^{-1}$). Higher concentrations (over 100 μg
43 kg^{-1}) were found in two areas: (i) close to the Alcudia coal-fired power plant; (ii) in the
44 city of La Palma. During the 11-year, the total Hg stock in Majorcan soil increased from
45 432.96 tons to 493.18 tones (14% increase). Based on a block kriging analysis, soil Hg
46 enrichment due to power plant emissions was clearly detectable on a local scale (i.e. a
47 shorter distance than 18 km from the power plant). Nonetheless, a significant island-
48 wide Hg increase due to diffuse pollution was reported. This result could be
49 extrapolated to other popular tourist destinations in the Mediterranean islands where
50 tourism has increased in recent decades In short, more than 60 tons of Hg have
51 accumulated on Majorca island in 11 years.

52

53 **Capsule**

54 Spatial patterns provided the first assessment of Hg stored trends on the entire Majorca
55 surface showed than 60 tons of Hg have accumulated on this island in 11 years

56

57 **Keywords:**

58 Soil Hg enriched; Spatial-temporal analysis; Coal-fired power plant; Hg pollution;
59 Mediterranean soil

60

61 **Highlights:**

- 62 - We analysed Hg soil spatial variability on the Majorca Island
- 63 - We found a high Hg concentration near the coal-fired power plant on Majorca
- 64 - We associate this effect with spatial patterns of Hg deposition on a local scale
- 65 - We found that most emitted Hg was deposited at distances less than 15 km
- 66 - We estimated that the Hg increase on the entire island in the last 11 years was 60 t

67

68

69

70 **1. INTRODUCTION**

71 Mercury (Hg) pollution is an environmental problem which, according to the World
72 Health Organization in 2017 (Raj and Maiti, 2019), poses a global threat. The UN's
73 International Chemical Safety Programme indicates that Hg is one of the six worst
74 pollutants on our planet (Keeler et al., 2006). Hg toxicity is associated with adverse
75 effects on most living organisms, including humans, especially neurological damage
76 (Beckers and Rinklebe, 2017; Wang et al., 2020; Zhang and Wong, 2007). Globally
77 accumulated Hg in soil is estimated to be 250–1,000 Gg (Raj and Maiti, 2019). Although
78 between 2,200 and 4,000 tons of Hg are emitted to the atmosphere every year (Wu et
79 al., 2016), about 60–80% of global Hg emissions come from anthropogenic sources
80 (Rodriguez Martin et al., 2014). According to O'Connor et al. (2019) anthropogenic
81 emissions of Hg to the environment being on the order of 2 Gg per year. Volatilization
82 from soil to atmosphere is considered transcendent (During et al., 2009; Rinklebe et al.,
83 2010) and soil temperature or soil water content are considered important factors on
84 dynamics of the total gaseous mercury (Rinklebe et al., 2010), although human
85 activities, such as fossil combustion (Kelepertzis and Argyraki, 2015b; Lv and Liu, 2019;
86 Rodriguez Martin et al., 2014), mining and smelting processes (Beckers and Rinklebe,
87 2017; Gutiérrez et al., 2016 ; Odumo et al., 2014), increase Hg levels in the environment,
88 but the most important sources of anthropogenic Hg emissions are coal-burning power
89 plants (Li et al., 2017; Raj and Maiti, 2019; Rodríguez Martín and Nanos, 2016).

90

91 The influence and repercussion of coal-fired power plants on atmospheric Hg
92 emissions are well-known (see "Mercury Falling" (Coequyt et al., 1999)). In fact coal-
93 burning power plants are the main source of Hg pollution (Wang et al., 2010; Yang and
94 Wang, 2008). Fossil fuel combustion represents approximately 60% of Hg emissions
95 worldwide (Pacyna et al., 2006) and 26% of all Hg emissions (236 tons/year) in
96 European electric energy plants (Pacyna et al., 2006). In Spain alone, coal-fired electric
97 power plants lie behind 47% of all Hg emissions (López Alonso et al., 2003). Some
98 studies (Streets et al., 2009) estimate that overall Hg emissions could increase to 96% by
99 2050 if new technologies are not set up to control coal-fired electric power plants. Hg
100 measurements in tree rings also show a continuous increase in atmospheric Hg levels
101 between 1975 and the present-day (Clackett et al., 2018). Conversely, research carried
102 out by EU GMOS (Global Mercury Observation System) estimate scenarios with an
103 85% reduction in Hg emissions by 2035 (Pacyna et al., 2016), which indicates a decrease

104 of up to 50% deposition in the Northern Hemisphere compared to 2013. This trend will
105 the result of the EU Mercury Strategy and the requirements set by the Minamata
106 Convention. It will agree with what the European Commission estimates for the future,
107 and with other research works that have indicated lowering Hg accumulation rates in
108 the last few decades (Corella et al., 2017) in the Western Mediterranean and fewer
109 anthropogenic Hg emissions in the past two decades in the Mediterranean Basin
110 (Cinnirella et al., 2019).

111

112 On the other hand, population growth increases atmospheric deposition due to urban
113 pollution (Mikayilov et al., 2019; Rodríguez Martín et al., 2015; Zhou and Wang, 2019).
114 This is especially relevant in areas where a disproportionate increase in tourists has
115 taken place in recent decades (Brtnický et al., 2020). Pollutants are directly associated
116 with tourism because energy use, construction of new infrastructures, transport and
117 other necessary services for tourists increase (Brtnický et al., 2020; Mikayilov et al.,
118 2019; Saenz-de-Miera and Rosselló, 2014). The Majorca Island (Spain) is a good study
119 area to evaluate possible environmental tourism impacts.

120

121 Majorca Island is one of the most popular tourist destinations in the Mediterranean
122 Region. It has a population of less than 1 million people, but was visited by 13.6 million
123 international tourists in 2019. For the Majorcan economy, although tourism generates
124 most revenue, it also contributes to increase air pollution. Due to the high numbers of
125 tourists, this demand makes a significant impact on environment. Saenz-de-Miera and
126 Rosselló (2014) showed that a 1% rise in tourist visits to Majorca increased PM₁₀ levels
127 by 0.45%. Given the global nature of the Hg problem, the UN Environment Programme
128 Minamata Convention (2017) includes provisions to reduce Hg emissions to the
129 atmosphere (Fisher and Nelson, 2020). However, the problem in most countries
130 underlies knowledge of Hg's sources and fate. In this regard, Coal-fired Thermal
131 Power Plant of Alcudia is the unique source of electricity production in the island.
132 Indeed soil is one of the most important reservoirs of Hg and can provide a record of
133 its deposition (Rodríguez Martín and Nanos, 2016). The Majorca Island (Spain) is also
134 good study area to evaluate the assumed Hg-enriched soil near the main coal-fired
135 power plant, where the effect of Hg pollution is limited to the entire island.

136 The main goals of this study were to: i) determine the Hg stock on the Majorca Island;
137 ii) analyse the spatial variability of soil Hg concentration in relation to the influence of

138 human activities and land use; iii) assess the temporal changes in soil Hg in soil after 11
139 years; iv) examine the Hg contamination level due to coal-fired power plant activity.

140

141 **2. MATERIALS AND METHODS**

142 **2.1 Study area**

143 The Majorca Island was traditionally an agricultural region located to the extreme west
144 of the Mediterranean Sea, whose climate is purely Mediterranean. The population of
145 Majorca island has slightly increased in 2017 (a population of 883 000) since 2006
146 (population 794 000). Agriculture has become less important while tourism has
147 developed in recent decades. In 2006 the number of tourists was 9.7 million, which
148 increased to 19.6 million in 2017. Nowadays, this island is an extremely popular
149 holiday destination, particularly for tourists from Germany and the UK. The
150 International Palma de Majorca Airport is the third busiest in Spain, and was used by
151 25 million passengers in 2016 (29 million in 2019). Tourism and urban development
152 have created a huge demand for services (food, energy, waste, rental vehicles, etc.) to
153 the detriment of environmental quality. Ecologists in Action report that The Balearics,
154 of which Majorca is the biggest island, has higher air pollution levels than those
155 recommended by the World Health Organization (WHO). Moreover, some 150,000
156 people (13% of the islands' population) live in areas where air pollution exceeds the
157 limits legally permitted in Spain
158 ([https://majorcadailybulletin.com/news/local/2016/10/27/45790/majorca-pollution-above-](https://majorcadailybulletin.com/news/local/2016/10/27/45790/majorca-pollution-above-recommended-levels.html)
159 [recommended-levels.html](https://majorcadailybulletin.com/news/local/2016/10/27/45790/majorca-pollution-above-recommended-levels.html)). Coal-fired Thermal Power Plant of Alcudia "Es Murterar" is
160 the "most polluting" facility in the Balearics, is responsible for 27% of CO₂ emissions. Es
161 Murterar power plant built in 1980 and later in 1997 it was expanded with one coal
162 group more with installed capacity above 130 MW. Currently, the partial closure of this
163 Power Plant is being considered as energy transition strategy.

164

165 **2.2 Sampling**

166 To evaluate the existing Hg concentration in soil on Majorca, 110 soil samples placed
167 on a regular grid design were collected on this island in 2016 and 2017 (Figure 1). For
168 each sampling site, at least 10 soil subsamples were taken from the upper 25 cm of soil.
169 Subsamples were thoroughly mixed in the field to select 3 kg of soil. In addition, rocky
170 fragments of ≥ 6 mm were taken to determine Hg contents in parent material. Twenty
171 eight of the 110 soil samples were established as sentinel plots (Figure 1), and occupied

172 the same locations where the 2006 field sampling was performed (Rodríguez Martín et
173 al., 2009c). The 2006 plots were selected according to a systematic grid (8 km × 8 km
174 size) on arable land (Rodríguez Martín et al., 2009c). The identical sampling and
175 laboratory methodology (see the next section) was followed for both sampling
176 campaigns to enable comparisons of Hg levels to be made over time without any
177 interferences from the field or laboratory methods. Other measurements taken at the
178 2016-17 sampling locations include:

- 179 • Two metal cores (400 cm³) per sampling site were driven in the top 20 cm of
180 soil. The extracted soil samples were transported to the lab to determine soil
181 bulk density (BD) and to obtain rocky fragments to evaluate stoniness
- 182 • Land-use classification of sampling locations. Sampling locations were
183 classified into one of the following land-use types: Forest (pine- or oak-
184 dominated), Annual crops, Fruit trees, Grassland, Wetland, Vineyard.

185

186 *Figure 1: Map of the Majorca Island showing the soil samples and the position of the Alcudia*
187 *coal-fired power plant.*

188

189 **2.3 Soil analytical methods**

190 Soil samples were air-dried and sieved to obtain two samples with rocky fragments of
191 > 6 mm and another sample of between 6 mm and 2 mm to determine coarse fragments
192 (% mineral particles > 2 mm in diameter), and to analyse Hg in rock. A fine soil sample
193 (< 2 mm) was used to establish Hg in topsoil. Bulk density was measured by the core
194 method (Black and Hartge, 1986). Soil organic matter (SOM) was analysed by the
195 Walkley-Black method. The total Hg in all the samples was determined by a direct Hg
196 analyser (DMA80) (Rodríguez Martín et al., 2009a). The limits of detection (LOD) and
197 quantification (LOQ) were 0.50 and 1.25 µg kg⁻¹, respectively. Certified calcareous loam
198 soil (BCR-141 R with 0.24±0.03 mg kg⁻¹ of total Hg) was employed for the analytical
199 procedure validation of soil samples. The Hg analysis revealed a good agreement
200 between the obtained and certified soil, and showed an average recovery of 98.7%.
201 Three replicates per sample were analysed.

202

203 **2.4 Statistical and geostatistical analyses**

204 Descriptive statistics were initially computed for the variables measured during the
205 2016-17 field campaign (Hg in soil, Hg in rocky fragments, BD, etc.). The hypothesis of

206 equality in the median Hg concentrations between different land-use types was tested
207 by the Kruskal-Wallis test. The null hypothesis of no year effect (i.e. 2006 vs. 2016-17)
208 was tested on the median Hg concentration of the 28 coincident samples by the same
209 statistical test.

210 Ordinary kriging (OK) with unique-global neighbourhood was used to generate
211 kriging maps on a squared grid of 100 x 100 m (1 ha cells) of the following variables:

- 212 • Hg concentration ($\mu\text{g}/\text{kg}$ of soil)
- 213 • Bulk density (g/cm^3)
- 214 • Fraction of coarse fragments (%)

215 To prepare the OK maps, spherical variogram models were adjusted to their
216 experimental counterparts. Variogram model parameters were estimated by an
217 iterative algorithm implemented in Isatis (Isatis, 2015). The estimation accuracy of the
218 kriging maps was assessed through cross-validation as described in Chilés and
219 Delfiner (1999). Briefly for cross-validation, two error indices were used to assess
220 kriging performance: (i) the mean error (E); (ii) the variance of the standardised error
221 ($Var(E_{st})$). With denoting Z and Z^* the observed and estimated value, respectively,
222 and σ the square root of kriging variance, the error indices can be written as:

$$223 \quad \bar{E} = \frac{1}{N} \sum_1^N (Z^* - Z)$$

$$224 \quad Var(E_{st}) = \frac{1}{N} \sum_1^N \left(\frac{Z^* - Z}{\sigma} \right)^2$$

225

226 **Estimating the Hg stock of Majorca in 2006 and 2016-17**

227 Let $i = 1, \dots$, then C denotes the i -th gridded cell on Majorca. The Hg stock (kg ha^{-1}) for
228 the i -th cell was calculated for each sampling campaign as:

$$229 \quad stock_{(i)} = Hg_{(i)} \times BD_{(i)} \times D \times (1 - S_{(i)})$$

230 where $Hg_{(i)}$ is the soil Hg concentration ($\mu\text{g kg}^{-1}$), $BD_{(i)}$ is BD (g cm^{-3}), $S_{(i)}$ is the
231 proportion of the volumetric coarse fragments fraction ($\text{g } 100^{-1}\text{g}$) of the i -th cell
232 estimated by the above-mentioned kriging procedure and D is soil layer thickness (25
233 cm). Finally, the average Hg stock was calculated as the average over the C cells of the
234 gridded map.

235

236 **2.5 Studying the effect of coal-fired power plant emissions on soil Hg**

237 To test the assumption of a distance-dependent effect of the Alcudia power plant on
238 Hg soil concentrations, block kriging (BK) was used. This method can be followed to

239 estimate the average pollutant concentration over a user-specified polygonal area. The
240 method is described in detail in several geostatistical textbooks (for instance, see Chilés
241 and Delfiner (1999)) and has been previously used in pollution case studies (Rodríguez
242 Martín et al., 2014; Rodríguez Martín and Nanos, 2016). Polygonal blocks (otherwise
243 polygons) were constructed using 16 concentric circles around the power plant with
244 variable radii from 3 km to 50 km. The intercircle polygonal areas (i.e. “rings”) were
245 then employed as blocks to estimate the average Hg concentration. Prior to
246 estimations, blocks were discretised into several small, non-overlapping rectangular
247 cells (100 m x 100 m cell size). Then BK was used to estimate the average Hg
248 concentration for each ring. Finally, 95% confidence intervals (95%CI) were estimated
249 for the block-average Hg concentration based on the estimated BK variance. The
250 kriging neighbourhood for estimating both the block-average Hg concentrations and
251 associated estimation variances was defined as “the soil samples lying within the ring
252 surface, plus the soil samples lying at a distance shorter than 6 km from the ring’s edge
253 in any direction”. The statistical analyses were carried out using the XLSTAT statistical
254 package (Addinsoft Version 2012.2.02), while ISATIS V10.0 and the Geostatistical
255 Analyst extension of ArcMap 10 were used for the geostatistical analyses.

256

257 **3. RESULTS AND DISCUSSION**

258 **3.1 Soil Hg concentrations and temporal changes in sentinel plots.**

259 The summary statistics of the Hg concentrations and soil parameters employed to
260 estimate Hg stock are listed in Table 1. No high concentrations were observed for the
261 Hg concentration in rocky fragments (mean 13.57 $\mu\text{g kg}^{-1}$). Hg concentrations tended
262 to be higher in the soils (mean 64.62 $\mu\text{g kg}^{-1}$) associated with some soil physico-
263 chemical properties, such as organic matter or clay contents (Gruba et al., 2019;
264 Kelepertzis and Argyraki, 2015a; Petrotou et al., 2012; Rodríguez Martín et al., 2009a),
265 but the levels in soil were 5-fold higher than lithogenic content. Mercury contaminated
266 soils constitute complex systems where many interdependent factors, including
267 amount and composition of soil organic matter and clays, oxidized minerals, reduced
268 elements, as well as soil pH and redox conditions affect Hg forms and transformation
269 (O'Connor et al., 2019). Nevertheless, the most important Hg input on the Majorca
270 Island can be associated with human activity. In fact in global terms, the largest Hg
271 contributions to the environment are attributed to human anthropogenic sources
272 (Kelepertzis and Argyraki, 2015b; Mirzaei et al., 2015; Raj and Maiti, 2019; Ravankhah

273 et al., 2017), mainly fossil fuel combustion (Beckers and Rinklebe, 2017; Botsou et al.,
274 2020; Fisher and Nelson, 2020; Pacyna et al., 2006).

275

276 *Table 1: Soil samples and statistical summary of the 2017 descriptive soil parameter sampling.*

277

278 The means soil Hg concentration in Majorcan soil (Tables 1 and 2) is similar to
279 mainland Spanish soil ($60 \mu\text{g kg}^{-1}$) (Rodríguez Martín et al., 2009c), but higher than
280 Europe topsoil Hg concentration ($22 \mu\text{g kg}^{-1}$) (Salminen et al., 2005). Other studies have
281 established an Hg background level of $20 \mu\text{g kg}^{-1}$ (Higuera et al., 2015) and a reference
282 value of $25 \mu\text{g kg}^{-1}$ (Gil et al., 2010) for the Spanish Mediterranean Region. This study
283 observed that 95% soil exceeded these levels. Annual crop soils (mean $70 \mu\text{g kg}^{-1}$)
284 presented maximum Hg concentration ($258 \mu\text{g kg}^{-1}$) (Table 2) in agricultural areas.
285 These high levels can be related to agricultural practices, and also to agrochemicals
286 being constantly incorporated into some annual vegetables crops, and often abusively
287 so (Ramos-Miras et al., 2019; Rodríguez Martín et al., 2013c). However, we were
288 surprised to also find high Hg concentrations in forest soil ($68 \mu\text{g kg}^{-1}$) and holm oaks,
289 or $69 \mu\text{g kg}^{-1}$ in pinewood (Table 2). These concentration levels in forest soil are higher
290 than for other agricultural soils on Majorca, which are associated with atmospheric
291 pollution (Hg air pollution).

292

293 *Table 2: Statistical summary of the Hg concentration in soil according to the land-use classes*
294 *sampling finished in 2017.*

295

296 Based on the Hg concentrations evaluated in the sentinel plots, the Hg concentration in
297 topsoil had increased after 11 years (Table 3). In 2006, the mean Hg concentration in
298 soil was $46.60 \mu\text{g kg}^{-1}$ compared to $62.10 \mu\text{g kg}^{-1}$ recorded in 2017 in the same plots.
299 Although this increase exceeds 30%, no clear differences were found to consider it to be
300 statistically significantly according to an ANOVA test. This finding suggests that the
301 observed increase was not homogeneous for the island on the whole, and it is also
302 necessary to consider that the variation in Hg soil concentration among crop types
303 (Table 2) might be more marked than the differences found between years. Therefore,
304 it was necessary to analyse Hg spatial variability in soil to be able to quantify the Hg
305 increase distribution and to locate possible pollution sources on this island.

306

307 *Table 3: Statistical summary of the Hg concentration ($\mu\text{g kg}^{-1}$) in the sentinel plots (28*
308 *samples)*

309

310 **3.2 Spatial variability and assessment of Hg stock on Majorca**

311 Experimental semivariograms are presented in the Supplementary Material (Figure
312 S1), where the exponential model was used to fit the semivariogram. The spatial
313 correlation range was significantly wider for BD (8 km) or stoniness (11 km) than for
314 Hg (4.1 km), which mainly represents the spatial variation corresponding to edaphic
315 influence and soil structure. Evidence for human influence can be associated with soil
316 Hg concentration due to a narrower spatial range than the mineralogical and bedrock
317 influences. Figure 2 shows the kriging map based on the semivariogram. The quality of
318 the prediction maps was examined by the cross-validation technique (Rodríguez
319 Martín et al., 2007). The mean errors and the root-mean-squared standardised errors
320 respectively came close to 0 and 1 (Table S1), which indicate the good accuracy of the
321 kriging maps. The Hg map indicated that some areas on the Majorca Island had high
322 concentration. This was particularly evidenced in the north-eastern part of the island,
323 which can associated with an industrial influence (Rodríguez Martín et al., 2013b)
324 related mainly to atmospheric deposition by the coal-burning power plant (Li et al.,
325 2017; Lv and Liu, 2019; Raj and Maiti, 2019; Rodríguez Martín and Nanos, 2016). In
326 addition, a small area to the east of the island near its capital also presented a high Hg
327 soil concentration. It is known that some urban activities are associated with Hg
328 pollution (Botsou et al., 2020; Trujillo-González et al., 2016; Zhou and Wang, 2019).
329 Higher stoniness percentages were recorded in the north and were associated mainly
330 with forest areas. The BD map showed a more homogeneous distribution with local
331 variation on the shorter scale related to soil compaction (Rodríguez Martín et al., 2016;
332 Trujillo-González et al., 2019).

333

334 *Figure S1: Experimental variogram and spatial models for mercury (Hg) concentration,*
335 *stoniness and bulk density (BD).*

336

337 *Figure 2: Spatial distribution of Hg concentration, stoniness and BD interpolated by ordinary*
338 *kriging.*

339

340 Hg stock (Figure 3) was computed as the product of three variables (Hg concentration,
341 BD and fraction of coarse fragments), which were regionalised by a geostatistical
342 approach. These maps showed Hg accumulation in soil. As we can see, the Hg stock on
343 the island generally increased, mainly in the northeast. In 2006, the highest Hg contents
344 were observed in the vicinity of the Alcudia coal-fired power point (Rodríguez Martín
345 et al., 2013b) where Hg accumulation was 4 g/ha. In 2017, Hg accumulation on the
346 island was more widely dispersed (Figure 3), although greater Hg accumulation was
347 still observed in the same area, and the highest levels had increased from 4.0 to 6.6
348 g/ha during the same 11-year period. The Hg stock 2017/Hg stock 2006 ratio was used
349 to identify these areas, which might suggest pollution inputs to evaluate temporal Hg
350 accumulation changes. Hg accumulation in this area was evidenced, where soil Hg
351 stock had tripled in only 11 years.

352 *Figure 3: Maps of the soil Hg stock on the Majorca Island. Values in kg ha⁻¹.*

353

354 This trend is not evidenced in our case, rather Hg stock in soil considerably increased
355 and does not only presently derive from the power plant, but also from diffuse
356 pollution on the island that is limited mostly to both its geographical area and
357 polluting activity on the island. Tourism pressure, and bigger summer populations
358 (Brtnický et al., 2020) with more than more than 13 million visitors in 2017, are
359 associated with services rendered to tourists, such as electricity, waste management,
360 incinerators, transport, rental vehicles, etc, which also play a key role in the rising Hg
361 levels on the island (Saenz-de-Miera and Rosselló, 2014). Growing populations and
362 cities are undoubtedly associated with more pollution (Kelepertzis and Argyraki,
363 2015b; Ravankhah et al., 2016; Rodríguez Martín et al., 2015; Trujillo-González et al.,
364 2016). Another area with a bigger Hg stock in soil is in the vicinity of the island's
365 capital (Palma de Majorca) as the contents quantified in 2006 had doubled in 2017.
366 Today Palma de Majorca has a population of 400,000 inhabitants, which is almost half
367 of the whole populating living on the island (907,000 people).

368

369 In short, the Hg stock for the Majorca Island on the whole has increased from 432.96
370 tons in 2006 to 493.18 tons in 2017 (Table 4). This means that more than 60 tons of Hg
371 have accumulated on the island in 11 years. For this same period, the mean Hg
372 deposition figure has been estimated at 33.40 $\mu\text{g m}^{-2} \text{ yr}^{-1}$. This value falls within the
373 wide range of deposition figures described by other studies. For example, Yu et al.

374 (2013) estimated Hg deposition to be $17.4 \mu\text{g m}^{-2} \text{yr}^{-1}$ in Adirondack Mountain (New
375 York State, USA) with wide variability (range from 3.7 to $46.0 \mu\text{g m}^{-2} \text{yr}^{-1}$). In
376 midcontinental North America (Wisconsin), Swain et al. (1992) quantified Hg
377 deposition to go from $3.7 \mu\text{g m}^{-2} \text{yr}^{-1}$ in 1,850 to $12.5 \mu\text{g m}^{-2} \text{yr}^{-1}$ in recent decades.
378 Wang et al. (2016) assessed global Hg deposition through litterfall, which they
379 estimated was $1,180 \pm 710 \text{ Mg yr}^{-1}$ and ranged from 2.7 to $219.9 \mu\text{g m}^{-2} \text{yr}^{-1}$ with a mean
380 of $27.4 \mu\text{g m}^{-2} \text{yr}^{-1}$, which is a similar estimate to that obtained herein. On Norwegian
381 land based on modelled deposition according to the European Monitoring and
382 Evaluation Programme (EMEP), Braaten et al. (2018) estimated a deposition flux of
383 only $9.5 \mu\text{g m}^{-2} \text{yr}^{-1}$. However, Steinnes et al. (1991) quantified $35 \mu\text{g m}^{-2} \text{yr}^{-1}$ near Oslo
384 (Norway). Navratil et al. (2019) evaluated Hg flux trends in the Czech Republic and
385 reported means of 45 and $32 \mu\text{g m}^{-2} \text{yr}^{-1}$, which lowered in forest soil from $66 \mu\text{g m}^{-2} \text{yr}^{-1}$
386 in 2003 to $23 \mu\text{g m}^{-2} \text{yr}^{-1}$ in 2017.

387 *Table 4: Soil mercury stock estimated from the kriging maps for 2006 and 2017.*

388 **3.3 Soil Hg and relations with pollution sources**

389 Soil Hg concentration depends primarily on geological parent material (soil-forming
390 factors) (Jimenez Ballesta, 2017; Papastergios et al., 2009; Rodríguez Martín et al.,
391 2009b). The rocky fragments of Hg content can be attributed only to the geochemical
392 processes that correspond to mineralogical structures (Rodríguez Martín et al., 2013a).
393 The Majorca Island is formed mostly by calcareous lithologies that were formed during
394 the Tertiary and do not present high concentration. The concentration ranges in the
395 rocky fragments on the Majorca Island fell between 5.70 and $20.50 \mu\text{g kg}^{-1}$ (mean 13.60
396 $\mu\text{g kg}^{-1}$) *versus* soil concentrations (mean $64.62 \mu\text{g kg}^{-1}$) (Table 1). The topsoil/rock Hg
397 content ratio has been used to evaluate soil Hg enrichment. Soil Hg is considered when
398 the metal concentration in soil is 8-fold higher than the litogenic content (Rodríguez
399 Martín et al., 2013b). Based on the assumption of a distance-dependent effect of coal-
400 fired power plant emissions on Hg soil concentrations, 16 concentric circles (radius of 3
401 km) centred on the Alcudia power plant were constructed and covered the whole
402 island surface (Figure 4). The mean Hg concentration in soil and the topsoil/rock ratio
403 between two consecutive areas (circles) were computed by BK (Rodríguez Martín et al.,
404 2014).

405

406 *Figure 4: Estimates of soil Hg and the soil/rock ratio computed by concentric circles in block*
407 *kriging and the associated confidence intervals around the Alcudia coal-fired power plant.*

408

409 The soil Hg concentration displayed a decreasing trend according to the distance to the
410 power plant (Figure 4). The highest mean concentration was observed in the second
411 ring (6 km) and the maximum ratio in the third ring (9 km), probably as a result of pipe
412 height preventing fly ash from being deposited on the power plant itself. Soil Hg was
413 15-fold higher than the lithogenic content near the power plant, which suggests major
414 local enrichment due to emissions. The Hg accumulation in the vicinity of power
415 plants has been reported in many studies (Li et al., 2017; Lv et al., 2019; Nóvoa-Muñoz
416 et al., 2008; Rodríguez Martín and Nanos, 2016; Yang and Wang, 2008) and is linked
417 with the carbon Hg content used in power plants (Rodríguez Martín et al., 2014; Wang
418 et al., 2010). These levels were higher according to the power plant energy capacity
419 (Nóvoa-Muñoz et al., 2008), especially in power plants over 1,000 MW (Rodríguez
420 Martín and Nanos, 2016). On Majorca, with a capacity to generate 218 MW, the
421 maximum soil Hg value was 258 $\mu\text{g kg}^{-1}$ (Table 1). On the Spanish mainland, soil
422 concentrations over 1,000 $\mu\text{g kg}^{-1}$ have been reported near similar coal combustion
423 power plants in Castellón (1650 MW), Aboño (921 MW) or Soto de Ribera (1481 MW)
424 (Rodríguez Martín and Nanos, 2016). Other studies have also reported soil
425 concentrations above 1,000 $\mu\text{g kg}^{-1}$ in the Baoji Power Plant of China (Yang and Wang,
426 2008), 1,600 $\mu\text{g kg}^{-1}$ in another Chinese power plant (Yuan et al., 2010) and 2,100 $\mu\text{g kg}^{-1}$
427 in the Serbian Nikola Tesla power plant (Dragović et al., 2013).

428

429 To summarise, coal-burning power plants are a relevant source of Hg emissions
430 (Coequyt et al., 1999; Furl and Meredith, 2011; Wang et al., 2010; Yang and Wang, 2008)
431 that often cause Hg enrichment in soils associated with atmospheric deposition (Li et
432 al., 2017; Lv et al., 2019; Rodríguez Martín et al., 2018). Hg volatilised during coal
433 combustion comes into contact with fly ash which, given its large specific area, is
434 finally enriched before escaping stack. This ash is deposited near power plants (Keeler
435 et al., 2006; Li et al., 2017; Rodríguez Martín et al., 2014). According to Figure 4, the
436 effect of the Alcudia coal-fired power plant on soil is limited to distances < 18 km,
437 which is a similar range to that observed in other studies (Li et al., 2017; Nanos et al.,
438 2015; Rodríguez Martín and Nanos, 2016). In this way, Hg concentrations in soil
439 increase compared to the contribution from weathering rocks. The present study shows
440 that the Alcudia power plant is the main local pollution source on the Majorca Island.
441 Its local influence on Hg soil concentration rapidly decreases with distance, but diffuse

442 pollution can affect the whole island by increasing Hg accumulation in soil through
443 atmospheric deposition.

444

445 **4 CONCLUSIONS**

446 Spatial patterns provided valuable information to quantify and evaluate Hg stock
447 trends. In line with the results of this study, we conclude that soil Hg levels have
448 substantially increased on the Majorca Island due to human activities. Interpolated
449 maps show that Hg concentration in topsoil has doubled in the vicinity of the Alcudia
450 coal-fired power plant in 11 years. Although the degree of pollution is high, spatial
451 patterns revealed that the most widely emitted Hg is deposited at distances less than
452 18 km. However, the effects of the Hg emissions from the coal-burning power plant are
453 stronger every year and Hg deposition can be hazardous in the future if a rising trend
454 persists.

455

456 A significant influence of tourism on the island's Hg contamination has been proved.
457 Population growth during holiday seasons increases atmospheric deposition by
458 rendering necessary services to tourists and related activities. In short, more than 60
459 tons of Hg have accumulated on this island in 11 years. Soil contamination on the
460 Majorca Island is expected to grow, which will have a negative impact on local
461 ecosystems. More environmental awareness is necessary in both the energy and
462 tourism sectors. According to the UN Sustainable Development Goals (SDG) and the
463 2020 Environmental Action Programme motto, "Living well, within the limits of our
464 planets" in the EU policy action, we hope that measures will be taken to conserve and
465 protect this island from increased pollution, which will involve taking actions to
466 reduce both the number of tourists and atmospheric deposition from the coal-fired
467 power plant. Presently certain technology, such as activated carbon injection, can
468 reduce emissions by 90%.

469

470

471 **5- ACKNOWLEDGEMENTS:**

472 We greatly appreciate the financial assistance provided by Spanish Ministry (Project
473 CGL2013-43675-P) and CAM (Project AGRISOST-CM S2018/BAA-4330).

474

475

476 **6- REFERENCES**

- 477 Beckers, F., Rinklebe, J., 2017. Cycling of mercury in the environment: Sources, fate,
478 and human health implications: A review. *Critical Reviews in Environmental*
479 *Science and Technology* 47, 693-794.
- 480 Black, G., Hartge, K., 1986. Bulk density. *Methods of soil analysis. Part 1*, 347-380.
- 481 Botsou, F., Moutafis, I., Dalaina, S., Kelepertzis, E., 2020. Settled bus dust as a proxy of
482 traffic-related emissions and health implications of exposures to potentially harmful
483 elements. *Atmospheric Pollution Research* 11, 1776-1784.
- 484 Braaten, H.F.V., Gundersen, C.B., Sample, J.E., Selvik, J.R., de Wit, H., 2018.
485 Atmospheric deposition and lateral transport of mercury in Norwegian drainage
486 basins: A mercury budget for Norway. NIVA-rapport.
- 487 Brtnický, M., Pecina, V., Galiová, M.V., Prokeš, L., Zvěřina, O., Juříčka, D., Klimánek,
488 M., Kynický, J., 2020. The impact of tourism on extremely visited volcanic island:
489 Link between environmental pollution and transportation modes. *Chemosphere*
490 249, 126118.
- 491 Cinnirella, S., Bruno, D.E., Pirrone, N., Horvat, M., Živković, I., Evers, D., Johnson, S.,
492 Sunderland, E., 2019. Mercury concentrations in biota in the Mediterranean Sea, a
493 compilation of 40 years of surveys. *Scientific data* 6, 1-11.
- 494 Clackett, S.P., Porter, T.J., Lehnerr, I., 2018. 400-year record of atmospheric mercury
495 from tree-rings in northwestern Canada. *Environmental Science & Technology* 52,
496 9625-9633.
- 497 Coequyt, J., Group, E.W., Council, N.R.D., Network, C.A., 1999. Mercury Falling: An
498 analysis of mercury pollution from coal-burning power plants. Environmental
499 Working Group.
- 500 Corella, J.P., Valero-Garcés, B.L., Wang, F., Martínez-Cortizas, A., Cuevas, C., Saiz-
501 Lopez, A., 2017. 700 years reconstruction of mercury and lead atmospheric
502 deposition in the Pyrenees (NE Spain). *Atmospheric Environment* 155, 97-107.
- 503 Chilés, J.P., Delfiner, P., 1999. *Geostatistics: Modeling Spatial Uncertainty*. John Wiley
504 & Sons, Inc, New York.
- 505 Dragović, S., Čujić, M., Slavković-Beškoski, L., Gajić, B., Bajat, B., Kilibarda, M., Onjia,
506 A., 2013. Trace element distribution in surface soils from a coal burning power
507 production area: A case study from the largest power plant site in Serbia. *CATENA*
508 104, 288-296.
- 509 During, A., Rinklebe, J., Boehme, F., Wennrich, R., Staerk, H.-J., Mothes, S., Du Laing,
510 G., Schulz, E., Neue, H.-U., 2009. Mercury volatilization from three floodplain soils
511 at the Central Elbe River, Germany. *Soil and Sediment Contamination* 18, 429-444
- 512 Fisher, J.A., Nelson, P.F., 2020. Atmospheric mercury in Australia: Recent findings and
513 future research needs. *Elementa: Science of the Anthropocene* 8.
- 514 Furl, C., Meredith, C., 2011. Mercury Accumulation in Sediment Cores from Three
515 Washington State Lakes: Evidence for Local Deposition from a Coal-Fired Power
516 Plant. *Archives of Environmental Contamination and Toxicology* 60, 26-33.
- 517 Gil, C., Ramos-Miras, J., Roca-Pérez, L., Boluda, R., 2010. Determination and
518 assessment of mercury content in calcareous soils. *Chemosphere* 78, 409-415.
- 519 Gruba, P., Socha, J., Pietrzykowski, M., Pasichnyk, D., 2019. Tree species affects the
520 concentration of total mercury (Hg) in forest soils: Evidence from a forest soil
521 inventory in Poland. *Science of The Total Environment* 647, 141-148.
- 522 Gutiérrez, C., Fernández, C., Escuer, M., Campos-Herrera, R., Beltrán Rodríguez, M.E.,
523 Carbonell, G., Rodríguez Martín, J.A., 2016. Effect of soil properties, heavy metals
524 and emerging contaminants in the soil nematodes diversity. *Environmental*
525 *Pollution* 213, 184-194.

526 Higuera, P., Fernández-Martínez, R., Esbrí, J., Rucandio, I., Loredó, J., Ordóñez, A.,
527 Álvarez, R., 2015. Mercury Soil Pollution in Spain: A Review, in: Jiménez, E.,
528 Cabañas, B., Lefebvre, G. (Eds.), *Environment, Energy and Climate Change I*.
529 Springer International Publishing, pp. 135-158.

530 Isatis, 2015. Isatis software manual. Geovariaciones & Ecole des Mines de Paris, Paris.

531 Jimenez Ballesta, R., 2017. *Introducción a la contaminación de suelos*. Mundi-Prensa
532 Libros.

533 Keeler, G.J., Landis, M.S., Norris, G.A., Christianson, E.M., Dvonch, J.T., 2006. Sources
534 of Mercury Wet Deposition in Eastern Ohio, USA. *Environmental Science &*
535 *Technology* 40, 5874-5881.

536 Kelepertzis, E., Argyraki, A., 2015a. Geochemical associations for evaluating the
537 availability of potentially harmful elements in urban soils: Lessons learnt from
538 Athens, Greece. *Applied Geochemistry* 59, 63-73.

539 Kelepertzis, E., Argyraki, A., 2015b. Mercury in the Urban Topsoil of Athens, Greece.
540 *Sustainability* 7, 4049-4062.

541 Li, R., Wu, H., Ding, J., Fu, W., Gan, L., Li, Y., 2017. Mercury pollution in vegetables,
542 grains and soils from areas surrounding coal-fired power plants. *Scientific Reports*
543 7, 46545.

544 López Alonso, M., Benedito, J.L., Miranda, M., Fernández, J.A., Castillo, C., Hernández,
545 J., Shore, R.F., 2003. Large-scale spatial variation in mercury concentrations in cattle
546 in NW Spain. *Environmental Pollution* 125, 173-181.

547 Lv, J., Liu, Y., 2019. An integrated approach to identify quantitative sources and
548 hazardous areas of heavy metals in soils. *Science of The Total Environment* 646, 19-
549 28.

550 Lv, J., Xia, Q., Yan, T., Zhang, M., Wang, Z., Zhu, L., 2019. Identifying the sources,
551 spatial distributions, and pollution status of heavy metals in soils from the southern
552 coast of Laizhou Bay, eastern China. *Human and Ecological Risk Assessment: An*
553 *International Journal* 25, 1953-1967.

554 Mikayilov, J.I., Mukhtarov, S., Mammadov, J., Azizov, M., 2019. Re-evaluating the
555 environmental impacts of tourism: does EKC exist? *Environmental Science and*
556 *Pollution Research* 26, 19389-19402.

557 Mirzaei, R., Teymourzade, S., Sakizadeh, M., Ghorbani, H., 2015. Comparative study of
558 heavy metals concentration in topsoil of urban green space and agricultural land
559 uses. *Environmental Monitoring and Assessment* 187, 741.

560 Nanos, N., Grigoratos, T., Rodríguez Martín, J., Samara, C., 2015. Scale-dependent
561 correlations between soil heavy metals and As around four coal-fired power plants
562 of northern Greece. *Stochastic Environmental Research and Risk Assessment* 29,
563 1531-1543.

564 Navrátil, T., Nováková, T., Roll, M., Shanley, J.B., Kopáček, J., Rohovec, J., Kaňa, J.,
565 Cudlín, P., 2019. Decreasing litterfall mercury deposition in central European
566 coniferous forests and effects of bark beetle infestation. *Science of The Total*
567 *Environment* 682, 213-225.

568 Nóvoa-Muñoz, J.C., Pontevedra-Pombal, X., Martínez-Cortizas, A., García-Rodeja
569 Gayoso, E., 2008. Mercury accumulation in upland acid forest ecosystems nearby a
570 coal-fired power-plant in Southwest Europe (Galicia, NW Spain). *Science of The*
571 *Total Environment* 394, 303-312.

572 O'Connor, D., Hou, D., Ok, Y.S., Mulder, J., Duan, L., Wu, Q., Wang, S., Tack, F.M.,
573 Rinklebe, J., 2019. Mercury speciation, transformation, and transportation in soils,
574 atmospheric flux, and implications for risk management: A critical review.
575 *Environment International* 126, 747-761.

576 Odumo, B., Carbonell, G., Angeyo, H., Patel, J., Torrijos, M., Rodríguez Martín, J., 2014.
577 Impact of gold mining associated with mercury contamination in soil, biota
578 sediments and tailings in Kenya. *Environmental Science and Pollution Research* 21,
579 12426-12435.

580 Pacyna, E.G., Pacyna, J.M., Fudala, J., Strzelecka-Jastrzab, E., Hlawiczka, S., Panasiuk,
581 D., 2006. Mercury emissions to the atmosphere from anthropogenic sources in
582 Europe in 2000 and their scenarios until 2020. *Science of The Total Environment* 370,
583 147-156.

584 Pacyna, J.M., Travnikov, O., Simone, F.d., Hedgecock, I.M., Sundseth, K., Pacyna, E.G.,
585 Steenhuisen, F., Pirrone, N., Munthe, J., Kindbom, K., 2016. Current and future
586 levels of mercury atmospheric pollution on a global scale.

587 Papastergios, G., Fernández-Turiel, J.-L., Georgakopoulos, A., Gimeno, D., 2009.
588 Natural and anthropogenic effects on the sediment geochemistry of Nestos River,
589 northern Greece. *Environmental Geology* 58, 1361-1370.

590 Petrotou, A., Skordas, K., Papastergios, G., Filippidis, A., 2012. Factors affecting the
591 distribution of potentially toxic elements in surface soils around an industrialized
592 area of northwestern Greece. *Environmental Earth Sciences* 65, 823-833.

593 Raj, D., Maiti, S.K., 2019. Sources, toxicity, and remediation of mercury: an essence
594 review. *Environmental Monitoring and Assessment* 191, 566.

595 Ramos-Miras, J.J., Gil, C., Rodríguez Martín, J.A., Bech, J., Boluda, R., 2019. Ecological
596 risk assessment of mercury and chromium in greenhouse soils. *Environmental*
597 *Geochemistry and Health*.

598 Ravankhah, N., Mirzaei, R., Masoum, S., 2016. Spatial eco-risk assessment of heavy
599 metals in the surface soils of industrial city of Aran-o-Bidgol, Iran. *Bulletin of*
600 *Environmental Contamination and Toxicology* 96, 516-523.

601 Ravankhah, N., Mirzaei, R., Masoum, S., 2017. Determination of heavy metals in
602 surface soils around the brick kilns in an arid region, Iran. *Journal of Geochemical*
603 *Exploration* 176, 91-99.

604 Rinklebe, J., Doring, A., Overesch, M., Du Laing, G., Wennrich, R., Stärk, H.-J., Mothes,
605 S., 2010. Dynamics of mercury fluxes and their controlling factors in large Hg-
606 polluted floodplain areas. *Environmental Pollution* 158, 308-318.

607 Rodríguez Martín, J., Carbonell Martín, G., López Arias, M., Grau Corbí, J., 2009a.
608 Mercury content in topsoils, and geostatistical methods to identify anthropogenic
609 input in the Ebro basin (Spain). *Spanish Journal of Agricultural Research* 7, 107-118.

610 Rodríguez Martín, J., Nanos, N., Grigoratos, T., Carbonell, G., Samara, C., 2014. Local
611 deposition of mercury in topsoils around coal-fired power plants: is it always true?
612 *Environmental Science and Pollution Research* 21, 10205-10214.

613 Rodríguez Martín, J., Nanos, N., Miranda, J., Carbonell, G., Gil, L., 2013a. Volcanic
614 mercury in *Pinus canariensis*. *Naturwissenschaften* 100, 739-747.

615 Rodríguez Martín, J., Vázquez de la Cueva, A., Grau Corbí, J., López Arias, M., 2007.
616 Factors Controlling the Spatial Variability of Copper in Topsoils of the Northeastern
617 Region of the Iberian Peninsula, Spain. *Water, Air, & Soil Pollution* 186, 311-321.

618 Rodríguez Martín, J., Vazquez de la Cueva, A., Grau Corbí, J., Martínez Alonso, C.,
619 López Arias, M., 2009b. Factors controlling the spatial variability of mercury
620 distribution in Spanish topsoil. *Soil & Sediment Contamination* 18, 30-42.

621 Rodríguez Martín, J.A., Álvaro-Fuentes, J., Gonzalo, J., Gil, C., Ramos-Miras, J.J., Grau
622 Corbí, J.M., Boluda, R., 2016. Assessment of the soil organic carbon stock in Spain.
623 *Geoderma* 264, Part A, 117-125.

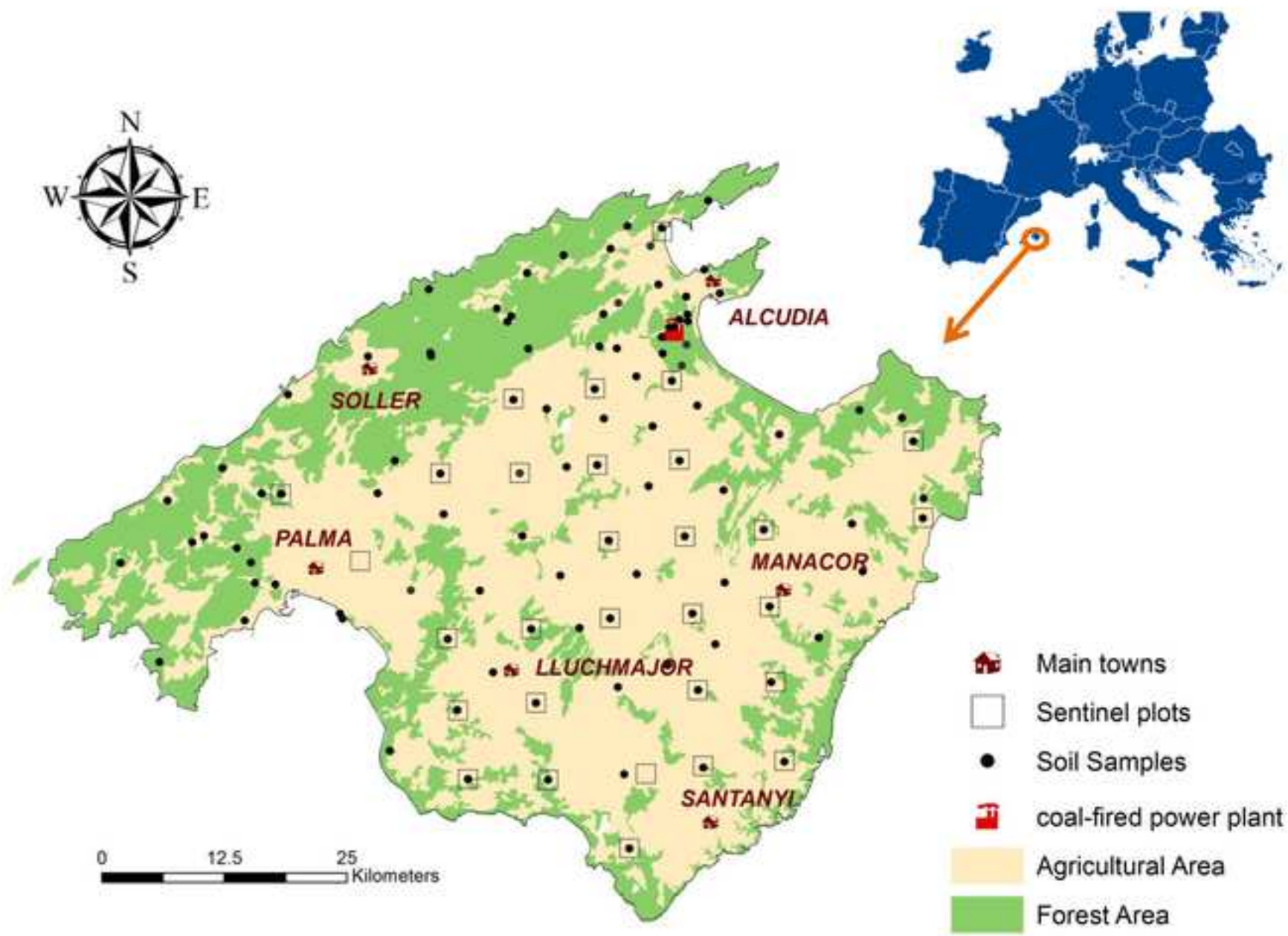
624 Rodríguez Martín, J.A., Carbonell, G., Nanos, N., Gutiérrez, C., 2013b. Source
625 Identification of Soil Mercury in the Spanish Islands. *Archives of Environmental*
626 *Contamination and Toxicology* 64, 171-179.

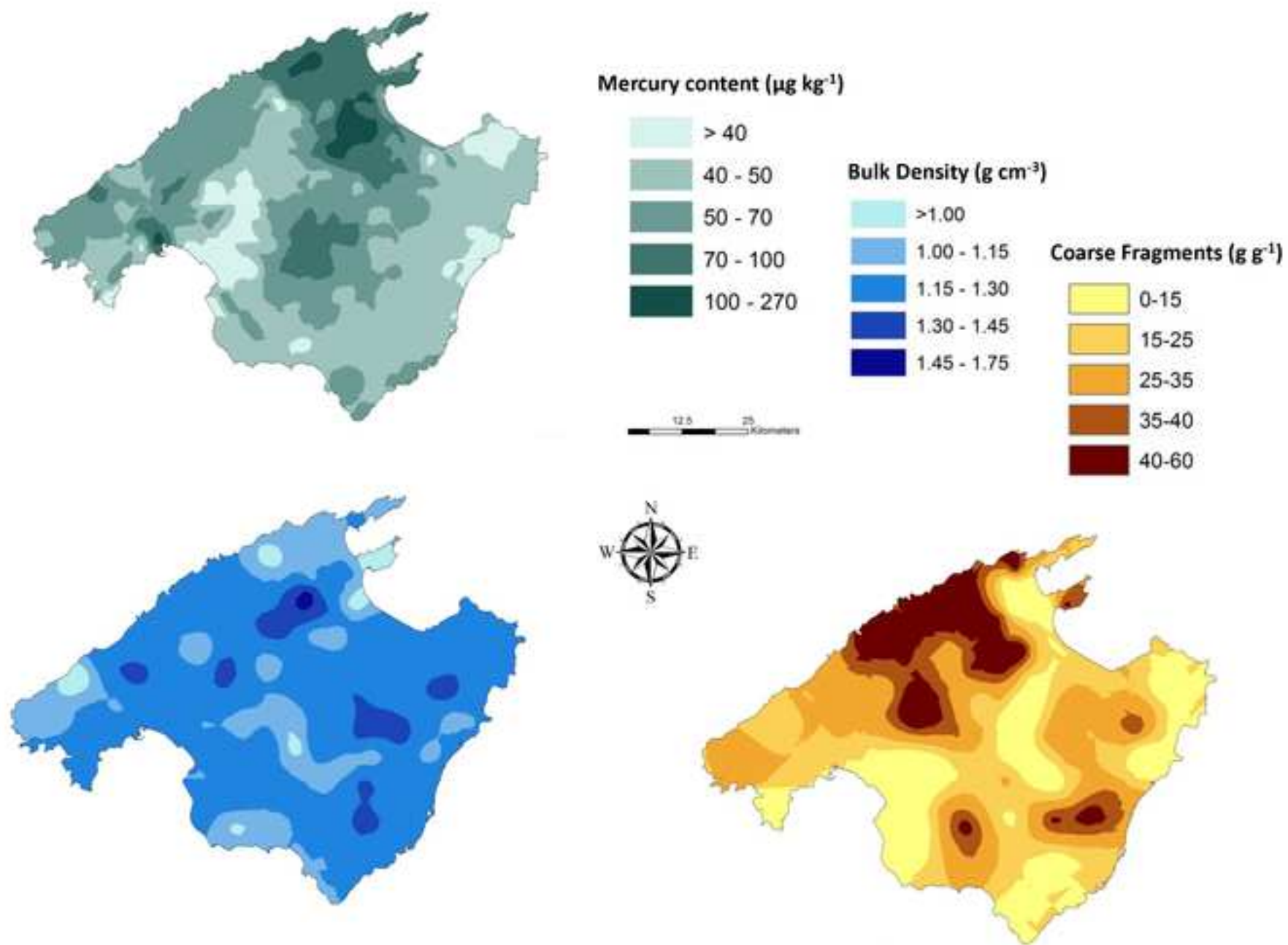
- 627 Rodríguez Martín, J.A., De Arana, C., Ramos-Miras, J.J., Gil, C., Boluda, R., 2015.
628 Impact of 70 years urban growth associated with heavy metal pollution.
629 Environmental Pollution 196, 156-163.
- 630 Rodríguez Martín, J.A., Gutiérrez, C., Torrijos, M., Nanos, N., 2018. Wood and bark of
631 Pinus halepensis as archives of heavy metal pollution in the Mediterranean Region.
632 Environmental Pollution 239, 438-447.
- 633 Rodríguez Martín, J.A., López Arias, M., Grau Corbí, J.M., 2009c. Metales pesados,
634 materia organica y otros parametros de los suelos agricolas y de pastos de España.
635 Ministerio de medio ambiente y medio rural y marino / Instituto Nacional de
636 Investigación y Tecnología Agraria y Alimentaria. , Madrid.
- 637 Rodríguez Martín, J.A., Nanos, N., 2016. Soil as an archive of coal-fired power plant
638 mercury deposition. Journal of Hazardous Materials 308, 131-138.
- 639 Rodríguez Martín, J.A., Ramos-Miras, J.J., Boluda, R., Gil, C., 2013c. Spatial relations of
640 heavy metals in arable and greenhouse soils of a Mediterranean environment region
641 (Spain). Geoderma 200–201, 180-188.
- 642 Saenz-de-Miera, O., Rosselló, J., 2014. Modeling tourism impacts on air pollution: The
643 case study of PM10 in Mallorca. Tourism Management 40, 273-281.
- 644 Salminen, R., Plant, J., Reeder, S., 2005. Geochemical atlas of Europe. Part 1,
645 Background information, methodology and maps. Geological survey of Finland.
- 646 Steinnes, E., Berg, T., Sjøbakk, T., 2003. Temporal and spatial trends in Hg deposition
647 monitored by moss analysis. Science of The Total Environment 304, 215-219.
- 648 Streets, D.G., Zhang, Q., Wu, Y., 2009. Projections of Global Mercury Emissions in 2050.
649 Environmental Science & Technology 43, 2983-2988.
- 650 Swain, E.B., Engstrom, D.R., Brigham, M.E., Henning, T.A., Brezonik, P.L., 1992.
651 Increasing rates of atmospheric mercury deposition in midcontinental North
652 America. Science 257, 784-787.
- 653 Trujillo-González, J.M., Torres-Mora, M.A., Jiménez-Ballesta, R., Zhang, J., 2019. Land-
654 use-dependent spatial variation and exposure risk of heavy metals in road-
655 deposited sediment in Villavicencio, Colombia. Environmental Geochemistry and
656 Health 41, 667-679.
- 657 Trujillo-González, J.M., Torres-Mora, M.A., Keesstra, S., Brevik, E.C., Jiménez-Ballesta,
658 R., 2016. Heavy metal accumulation related to population density in road dust
659 samples taken from urban sites under different land uses. Science of The Total
660 Environment 553, 636-642.
- 661 Wang, L., Hou, D., Cao, Y., Ok, Y.S., Tack, F.M.G., Rinklebe, J., O'Connor, D., 2020.
662 Remediation of mercury contaminated soil, water, and air: A review of emerging
663 materials and innovative technologies. Environment International 134, 105281.
- 664 Wang, S., Zhang, L., Li, G., Wu, Y., Hao, J., Pirrone, N., Sprovieri, F., Ancora, M., 2010.
665 Mercury emission and speciation of coal-fired power plants in China. Atmospheric
666 Chemistry and Physics 10, 1183-1192.
- 667 Wang, X., Bao, Z., Lin, C.-J., Yuan, W., Feng, X., 2016. Assessment of global mercury
668 deposition through litterfall. Environmental Science & Technology 50, 8548-8557.
- 669 Wu, Q., Wang, S., Li, G., Liang, S., Lin, C.-J., Wang, Y., Cai, S., Liu, K., Hao, J., 2016.
670 Temporal trend and spatial distribution of speciated atmospheric mercury
671 emissions in China during 1978–2014. Environmental Science & Technology 50,
672 13428-13435.
- 673 Yang, X., Wang, L., 2008. Spatial analysis and hazard assessment of mercury in soil
674 around the coal-fired power plant: a case study from the city of Baoji, China.
675 Environmental Geology 53, 1381-1388.

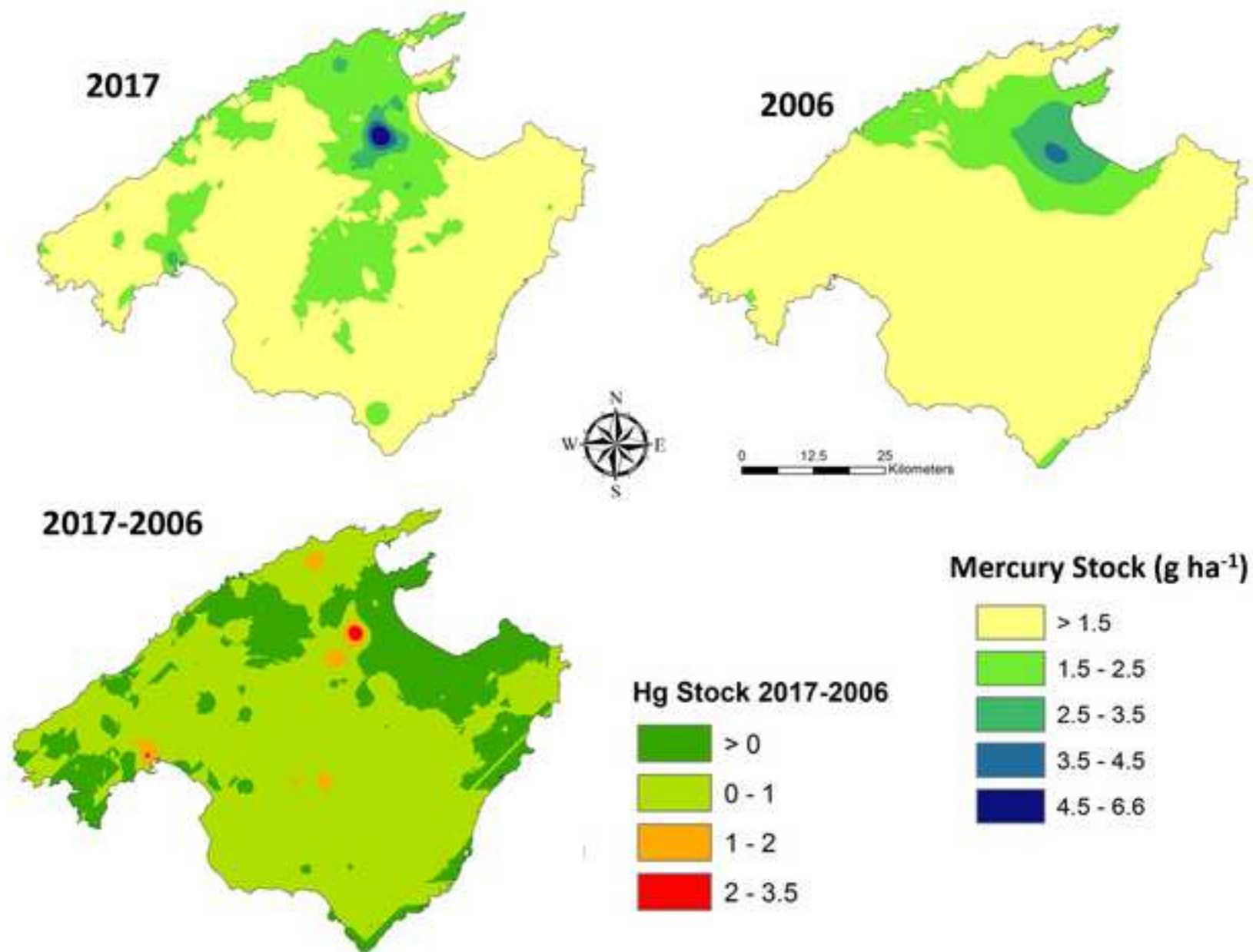
- 676 Yu, X., Driscoll, C.T., Huang, J., Holsen, T.M., Blackwell, B.D., 2013. Modeling and
677 mapping of atmospheric mercury deposition in Adirondack Park, New York. PLoS
678 ONE 8.
- 679 Yuan, C.-G., Wang, T.-F., Song, Y.-F., Chang, A.-L., 2010. Total mercury and
680 sequentially extracted mercury fractions in soil near a coal-fired power plant.
681 Fresenius Environmental Bulletin 19, 2857-2863.
- 682 Zhang, L., Wong, M., 2007. Environmental mercury contamination in China: sources
683 and impacts. Environment International 33, 108-121.
- 684 Zhou, X.-Y., Wang, X.-R., 2019. Impact of industrial activities on heavy metal
685 contamination in soils in three major urban agglomerations of China. Journal of
686 Cleaner production 230, 1-10.

687

Figure 1







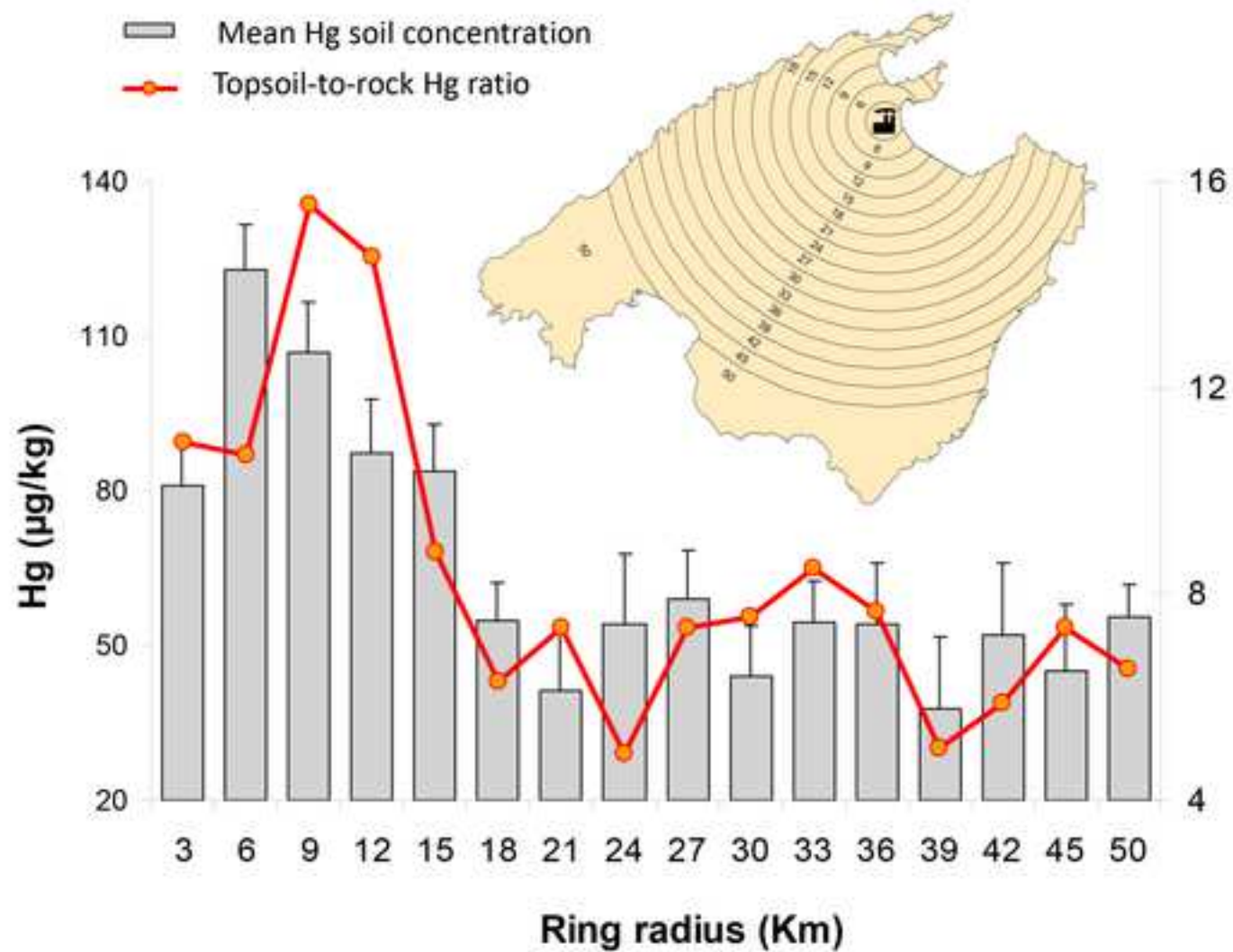


Table 1: Soil samples and statistical summary of the 2017 descriptive soil parameter sampling.

Soil parameter	No. Samples	Mean	Median	SD	Min	Max	3rd Qu
Topsoil Hg ($\mu\text{g kg}^{-1}$)	107	64.62	52.39	36.87	13.85	258.04	78.40
Bulk density (BD)	89	1.181	1.180	0.169	0.655	1.691	1.290
Stoniness (%)	89	25.80	22.98	15.01	2.42	59.73	34.08
Rock Hg ($\mu\text{g kg}^{-1}$)	86	13.57	8.32	13.14	1.62	71.14	16.37
SOC (%C)	110	2.62	2.00	1.83	0.81	12.51	3.19

Table 2: Statistical summary of the Hg concentration in soil according to the land-use classes sampling finished in 2017.

Landuse	No. Samples	Mean	Median	SD	Min	Max	3rd Qu
Annual crops	31	70.25	58.10	45.83	24.18	258.04	80.52
Fruit trees	19	55.19	48.29	21.84	20.55	100.54	69.15
Vineyard	2	33.69	33.69	10.86	26.01	41.37	37.53
Grassland	10	57.48	44.73	32.39	33.90	142.89	61.83
Forest (holm oak)	9	68.41	77.95	32.84	31.12	128.06	87.03
Forest (pinewood)	32	69.40	59.58	38.98	13.85	162.12	97.15
Wetland (natural Park)	4	53.74	47.67	22.94	33.61	86.01	61.32

Qu quartile; SD standard deviation.

Table 3: Statistical summary of the Hg concentration ($\mu\text{g kg}^{-1}$) in the sentinel plots (28 samples)

	2006	2016	Significant differences
Mean	46.58	62.09	P=0.161 (ANOVA). ns
Median	39.33	47.27	P=0.026 (Kruskal–Wallis test).*
SD	38.75	42.86	
Min.	17.33	20.55	
Max.	229.53	226.60	
3rd Qu	52.42	72.43	

Significant differences between years are shown in Medians (Kruskal–Wallis test), no differences are observed between the means (ANOVA test).

Table 4: Soil mercury stock estimated from the kriging maps for 2006 and 2017.

	2017	2006
Mean (kg/ha)	1.36	1.20
SD	0.45	0.55
Min	0.39	0.54
Max	6.67	4.06
Total Hg Stock (tons)	493.18	432.96

Total island surface is 3620km² (362043 ha). Temporary change in the total stock is estimated in 60.2 tons

Declaration of interests


The authors declare that they have no known competing financial interests or personal relationships that could have appeared to influence the work reported in this paper.

The authors declare the following financial interests/personal relationships which may be considered as potential competing interests:


CRedit author statement

José Antonio Rodríguez Martín: Conceptualization, Methodology, Writing, Writing - Review & Editing, Supervision. **Carmen Gutiérrez:** Conceptualization, Methodology, Writing, Funding acquisition. **Miguel Escuer:** Methodology, Writing, Investigation. **Marina Martín-Dacal:** Methodology, Writing, Investigation. **José Joaquín Ramos-Miras:** Validation, Writing, Investigation. **Luis Roca-Perez:** Validation, Writing, Investigation. **Rafael Boluda:** Validation, Writing, Investigation. **Nikos Nanos:** Formal analysis, Methodology, Investigation, Software

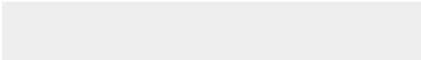

.



Click here to access/download
Supplementary Material
Figure S1.jpg



Click here to access/download
Supplementary Material
Table S1 revised.docx



1 **Trends in soil mercury stock associated with pollution sources on a**
2 **Mediterranean island (Majorca, Spain)**

3

4 Authors: José Antonio Rodríguez Martín ^{(1)*}, Carmen Gutiérrez ⁽²⁾, Miguel Escuer ⁽²⁾,
5 Marina Martín-Dacal ⁽³⁾, José Joaquín Ramos-Miras ⁽⁴⁾, Luis Roca-Perez ⁽⁵⁾, Rafael
6 Boluda ⁽⁵⁾, Nikos Nanos ⁽⁶⁾.

7

8 ¹ Department of Environment, Instituto Nacional de Investigación y Tecnología Agraria y
9 Alimentaria (INIA), ES-28040, Madrid, Spain. (e-mail: rmartin@inia.es)

10 ² Instituto de Ciencias Agrarias, ICA- CSIC. Serrano, 114bis. 28006 Madrid, Spain. (e-mail:
11 carmen.g@ica.csic.es)

12 ³ Centro de Biotecnología y Genómica de Plantas (UPM-INIA). Parque Científico y Tecnológico,
13 UPM Campus de Montegancedo, 28223 Madrid, Spain (e-mail: marina.md96@gmail.com)
14 marina.martind@upm.es

15 ⁴ Dpto. Didáctica Ciencias Sociales y Experimentales, Universidad de Córdoba, Avda. San
16 Alberto Magno s/n, Córdoba 14071, Spain. (e-mail: jjramos@uco.es)

17 ⁵ Dept. Biología Vegetal, Facultat de Farmàcia, Universitat de València, Av. Vicent Andrés i
18 Estellés s/n, 46100 Burjassot, (Valencia), Spain (e-mail: boluda@uv.es)

19 ⁶ School of Forestry and Natural Environment, Aristotle University of Thessaloniki. 59
20 Moschounti str., 55134 Foinikas-Thessaloniki, Greece. (e-mail: nikosnanos@for.auth.gr)

21

22

23 *Corresponding author: e-mail: rmartin@inia.es

24 Telephone/fax number: -34 913476795/ +34 913474008

25

26

27

28

29

30

31

32

33

34

35

36 Abstract

37 ~~Mercury~~Hg is a global concern given its adverse effects on human health, food security
38 and the environment, and it requiring actions to identify major local Hg sources and to
39 evaluate pollution. Our study provides the first assessment of Hg stock trends on the
40 entire Majorca surface, identifying~~We identified~~ major Hg sources ~~on the Majorca~~
41 ~~Island~~ by studying the spatiotemporal soil Hg variation at two successive times (2006
42 and 2016-17). The Hg soil concentration ranged from 14 to 258 $\mu\text{g kg}^{-1}$ (mean 52.40 μg
43 kg^{-1}). Higher concentrations (over 100 $\mu\text{g kg}^{-1}$) were found in three-two areas: (i) close
44 to the Alcudia coal-fired power plant; (ii) in the city of Lla Palma; ~~in the northeastern~~
45 ~~forest areas of this island~~. During the 11-year ~~period between samplings~~, the total Hg
46 stock in Majorcan soil increased from 432.96 tons to 493.18 tones (14% increase). Based
47 on a block kriging analysis, soil Hg enrichment due to power plant emissions was
48 clearly detectable on a local scale (i.e. a shorter distance than 18 km from the power
49 plant). Nonetheless, ~~the present study also highlights~~ a significant island-wide Hg
50 increase ~~in soil Hg content~~ due to diffuse pollution was reported. This result could be
51 extrapolated to other popular tourist destinations in the Mediterranean islands where
52 tourism has increased in recent decades motivated by increased tourism. In short, more
53 than 60 tons of Hg have accumulated on Majorca island in 11 years.

54

55 Capsule

56 Spatial patterns provided the first assessment of Hg stored trends on the entire Majorca
57 surface showed than 60 tons of Hg have accumulated on this island in 11 years

58

59 Keywords:

60 Soil ~~mercury~~Hg enriched; Spatial-temporal analysis; Coal-fired power plant;
61 ~~Mercury~~Hg pollution; Mediterranean soil

62

63 Highlights:

- 64 - We analysed Hg soil spatial variability on the Majorca Island
- 65 - We found a high Hg ~~content~~concentration near the coal-fired power plant on Majorca
- 66 - We associate this effect with spatial patterns of Hg deposition on a local scale
- 67 - We found that most emitted ~~mercury~~Hg was deposited at distances less than 15 km
- 68 - We estimated that the Hg increase on the entire island in the last 11 years was 60 t

69

70

71

72 1. INTRODUCTION

73 Mercury (Hg) pollution is an environmental problem which, according to the World
74 Health Organization in 2017 (Raj and Maiti, 2019), poses a global threat. The UN's
75 International Chemical Safety Programme indicates that Hg is one of the six worst
76 pollutants on our planet (Keeler et al., 2006). Hg toxicity is associated with adverse
77 effects on most living organisms, including humans, especially neurological damage
78 (Beckers and Rinklebe, 2017; Wang et al., 2020; Zhang and Wong, 2007). Globally
79 accumulated Hg in soil is estimated to be 250–1,000 Gg (Raj and Maiti, 2019). Although
80 between 2,200 and 4,000 tons of Hg are emitted to the atmosphere every year (Wu et
81 al., 2016), about 60–80% of global Hg emissions come from anthropogenic sources
82 (Rodríguez Martín et al., 2014). According to O'Connor et al. (2019) anthropogenic
83 emissions of Hg to the environment being on the order of 2 Gg per year. Volatilization
84 from soil to atmosphere is considered transcendent (During et al., 2009; Rinklebe et al.,
85 2010) and -soil temperature or soil water content are considered important factors on
86 dynamics of the total gaseous mercury (Rinklebe et al., 2010), although Hhuman
87 activities, such as fossil combustion (Kelepertzis and Argyraki, 2015b; Lv and Liu, 2019;
88 Rodríguez Martín et al., 2014), mining and smelting processes (Beckers and Rinklebe,
89 2017; Gutiérrez et al., 2016 ; Odumo et al., 2014), increase Hg levels in the environment,
90 but the most important sources of anthropogenic Hg emissions are coal-burning power
91 plants (Li et al., 2017; Raj and Maiti, 2019; Rodríguez Martín and Nanos, 2016).

92

93 The influence and repercussion of coal-fired power plants on atmospheric Hg
94 emissions are well-known (see "Mercury Falling" (Coequyt et al., 1999)). In fact coal-
95 burning power plants are the main source of Hg pollution (Wang et al., 2010; Yang and
96 Wang, 2008). Fossil fuel combustion represents approximately 60% of Hg emissions
97 worldwide (Pacyna et al., 2006) and 26% of all Hg emissions (236 tons/year) in
98 European electric energy plants (Pacyna et al., 2006). In Spain alone, coal-fired electric
99 power plants lie behind 47% of all Hg emissions (López Alonso et al., 2003). Some
100 studies (Streets et al., 2009) estimate that overall Hg emissions could increase to 96% by
101 2050 if new technologies are not set up to control coal-fired electric power plants. Hg
102 measurements in tree rings also show a continuous increase in atmospheric Hg levels
103 between 1975 and the present-day (Clackett et al., 2018). Conversely, research carried
104 out by EU GMOS (Global Mercury Observation System) estimate scenarios with an
105 85% reduction in Hg emissions by 2035 (Pacyna et al., 2016), which indicates a decrease

106 of up to 50% deposition in the Northern Hemisphere compared to 2013. This trend will
107 the result of the EU Mercury Strategy and the requirements set by the Minamata
108 Convention. It will agree with what the European Commission estimates for the future,
109 and with other research works that have indicated lowering Hg accumulation rates in
110 the last few decades (Corella et al., 2017) in the Western Mediterranean and fewer
111 anthropogenic Hg emissions in the past two decades in the Mediterranean Basin
112 (Cinnirella et al., 2019).

113
114 On the other hand,

115 Population growth increases atmospheric deposition due to urban pollution
116 (Mikayilov et al., 2019; Rodríguez Martín et al., 2015; Zhou and Wang, 2019). This is
117 especially relevant in areas where a disproportionate increase in tourists has taken
118 place in recent decades (Brtnický et al., 2020). Pollutants are directly associated with
119 tourism because energy use, construction of new infrastructures, transport and other
120 necessary services for tourists increase (Brtnický et al., 2020; Mikayilov et al., 2019;
121 Saenz-de-Miera and Rosselló, 2014). The Majorca Island (Spain) is a good study area to
122 evaluate possible environmental tourism impacts.

123
124 Majorca ~~This island~~ Island is one of the most popular tourist destinations in the
125 Mediterranean Region. It has a population of less than 1 million people, but was visited
126 by 13.6 million international tourists in 2019. For the Majorcan economy, although
127 tourism generates most revenue, it also contributes to increase air pollution. Due to the
128 high numbers of tourists, this demand makes a significant impact on environment.
129 Saenz-de-Miera and Rosselló (2014) showed that a 1% rise in tourist visits to Majorca
130 increased PM₁₀ levels by 0.45%. Given the global nature of the Hg problem, the UN
131 Environment Programme Minamata Convention (2017) includes provisions to reduce
132 Hg emissions to the atmosphere (Fisher and Nelson, 2020). However, the problem in
133 most countries underlies knowledge of Hg's sources and fate. In this regard, Coal-fired
134 Thermal Power Plant of Alcudia is the unique source of electricity production in the
135 island. Indeed soil is one of the most important reservoirs of Hg and can provide a
136 record of its deposition (Rodríguez Martín and Nanos, 2016). The Majorca Island
137 (Spain) is also good study area to evaluate the assumed Hg-enriched soil near the main
138 coal-fired power plant, where the effect of Hg pollution is limited to the entire island.

140 The main goals of this study were to: i) determine the Hg stock on the Majorca Island;
141 ii) analyse the spatial variability of soil Hg ~~content~~concentration in relation to the
142 influence of human activities and land use; iii) assess the temporal changes in soil Hg
143 in soil after 11 years; iv) examine the Hg contamination level due to coal-fired power
144 plant activity.

145

146 2. MATERIALS AND METHODS

147 2.1 Study area

148 The Majorca Island was traditionally an agricultural region located to the extreme west
149 of the Mediterranean Sea, whose climate is purely Mediterranean. The population of
150 Majorca island has slightly increased in 2017 (a population of 883 000) since 2006
151 (population 794 000). Agriculture has become less important while tourism has
152 developed in recent decades. In 2006 the number of tourists was 9.7 million, which
153 increased to 19.6 million in 2017. Nowadays, this island is an extremely popular
154 holiday destination, particularly for tourists from Germany and the UK. The
155 International Palma de Majorca Airport is the third busiest in Spain, and was used by
156 25 million passengers in 2016 (29 million in 2019). Tourism and urban development
157 have created a huge demand for services (food, energy, waste, rental vehicles, etc.) to
158 the detriment of environmental quality. Ecologists in Action report that The Balearics,
159 of which Majorca is the biggest island, has higher air pollution levels than those
160 recommended by the World Health Organization (WHO). Moreover, some 150,000
161 people (13% of the islands' population) live in areas where air pollution exceeds the
162 limits legally permitted in Spain
163 ([https://majorcadailybulletin.com/news/local/2016/10/27/45790/majorca-pollution-above-](https://majorcadailybulletin.com/news/local/2016/10/27/45790/majorca-pollution-above-recommended-levels.html)
164 [recommended-levels.html](https://majorcadailybulletin.com/news/local/2016/10/27/45790/majorca-pollution-above-recommended-levels.html)). Coal-fired Thermal Power Plant of Alcudia
165 "Es Murterar" is the "most polluting" facility in the Balearics, is responsible for 27% of
166 CO₂ emissions. Es Murterar power plant built in 1980 and later in 1997 it was expanded
167 with one coal group more with installed capacity above 130 MW. Currently, the partial
168 closure of this Power Plant is being considered as energy transition strategy.

169

170 2.2 Sampling

171 To evaluate the existing Hg concentration in soil on Majorca, 110 soil samples placed
172 on a regular grid design were collected on this island in 2016 and 2017 (Figure 1). For
173 each sampling site, at least 10 soil subsamples were taken from the upper 25 cm of soil.

174 Subsamples were thoroughly mixed in the field to select 3 kg of soil. In addition, rocky
175 fragments of ≥ 6 mm were taken to determine Hg contents in parent material. Twenty
176 eight of the 110 soil samples were established as sentinel plots (Figure 1), and occupied
177 the same locations where the 2006 field sampling was performed (Rodríguez Martín et
178 al., 2009c). The 2006 plots were selected according to a systematic grid (8 km \times 8 km
179 size) on arable land (Rodríguez Martín et al., 2009c). The identical sampling and
180 laboratory methodology (see the next section) was followed for both sampling
181 campaigns to enable comparisons of Hg levels to be made over time without any
182 interferences from the field or laboratory methods. Other measurements taken at the
183 2016-17 sampling locations include:

- 184 • Two metal cores (400 cm³) per sampling site were driven in the top 20 cm of
185 soil. The extracted soil samples were transported to the lab to determine soil
186 bulk density (BD) and to obtain rocky fragments to evaluate stoniness
- 187 • Land-use classification of sampling locations. Sampling locations were
188 classified into one of the following land-use types: Forest (pine- or oak-
189 dominated), Annual crops, Fruit trees, Grassland, Wetland, Vineyard.

190

191 *Figure 1: Map of the Majorca Island showing the soil samples and the position of the Alcudia*
192 *coal-fired power plant.*

193

194 **2.3 Soil analytical methods**

195 Soil samples were air-dried and sieved to obtain two samples with rocky fragments of
196 > 6 mm and another sample of between 6 mm and 2 mm to determine coarse fragments
197 (% mineral particles > 2 mm in diameter), and to analyse Hg in rock. A fine soil sample
198 (< 2 mm) was used to establish Hg in topsoil. Bulk density was measured by the core
199 method (Black and Hartge, 1986). Soil organic matter (SOM) was analysed by the
200 Walkley-Black method. The total Hg in all the samples was determined by a direct Hg
201 analyser (DMA80) (Rodríguez Martín et al., 2009a). The limits of detection (LOD) and
202 quantification (LOQ) were 0.50 and 1.25 $\mu\text{g kg}^{-1}$, respectively. Certified calcareous loam
203 soil (BCR-141 R with 0.24 ± 0.03 $\mu\text{g kg}^{-1}$ of total Hg) was employed for the analytical
204 procedure validation of soil samples. The Hg analysis revealed a good agreement
205 between the obtained and certified soil, and showed an average recovery of 98.7%.
206 Three replicates per sample were analysed.

207

208 2.4 Statistical and geostatistical analyses

209 Descriptive statistics were initially computed for the variables measured during the
210 2016-17 field campaign (Hg in soil, Hg in rocky fragments, BD, etc.). The hypothesis of
211 equality in the median Hg concentrations between different land-use types was tested
212 by the Kruskal-Wallis test. The null hypothesis of no year effect (i.e. 2006 vs. 2016-17)
213 was tested on the median Hg concentration of the 28 coincident samples by the same
214 statistical test.

215 Ordinary kriging (OK) with unique-global neighbourhood was used to generate
216 kriging maps on a squared grid of 100 x 100 m (1 ha cells) of the following variables:

- 217 • Hg concentration ($\mu\text{g}/\text{kg}$ of soil)
- 218 • Bulk density (g/cm^3)
- 219 • Fraction of coarse fragments (%)

220 To prepare the OK maps, spherical variogram models were adjusted to their
221 experimental counterparts. Variogram model parameters were estimated by an
222 iterative algorithm implemented in Isatis (Isatis, 2015). The estimation accuracy of the
223 kriging maps was assessed through cross-validation as described in Chilés and
224 Delfiner (1999). Briefly for cross-validation, two error indices were used to assess
225 kriging performance: (i) the mean error (E); (ii) the variance of the standardised error
226 ($\text{Var}(E_{st})$). With denoting Z and Z^* the observed and estimated value, respectively,
227 and σ the square root of kriging variance, the error indices can be written as:

$$228 \quad \bar{E} = \frac{1}{N} \sum_{i=1}^N (Z^* - Z)$$

$$229 \quad \text{Var}(E_{st}) = \frac{1}{N} \sum_{i=1}^N \left(\frac{Z^* - Z}{\sigma} \right)^2$$

230

231 Estimating the Hg stock of Majorca in 2006 and 2016-17

232 Let $i = 1, \dots$, then C denotes the i -th gridded cell on Majorca. The Hg stock (kg ha^{-1}) for
233 the i -th cell was calculated for each sampling campaign as:

$$234 \quad \text{stock}_{(i)} = Hg_{(i)} \times BD_{(i)} \times D \times (1 - S_{(i)})$$

235 where $Hg_{(i)}$ is the soil Hg concentration ($\mu\text{g kg}^{-1}$), $BD_{(i)}$ is BD (g cm^{-3}), $S_{(i)}$ is the
236 proportion of the volumetric coarse fragments fraction ($\text{g } 100^{-1}\text{g}$) of the i -th cell
237 estimated by the above-mentioned kriging procedure and D is soil layer thickness (25
238 cm). Finally, the average Hg stock was calculated as the average over the C cells of the
239 gridded map.

240

241 2.5 Studying the effect of coal-fired power plant emissions on soil Hg

242 To test the assumption of a distance-dependent effect of the Alcudia power plant on
243 Hg soil concentrations, block kriging (BK) was used. This method can be followed to
244 estimate the average pollutant concentration over a user-specified polygonal area. The
245 method is described in detail in several geostatistical textbooks (for instance, see Chilés
246 and Delfiner (1999)) and has been previously used in pollution case studies (Rodríguez
247 Martín et al., 2014; Rodríguez Martín and Nanos, 2016). Polygonal blocks (otherwise
248 polygons) were constructed using 16 concentric circles around the power plant with
249 variable radii from 3 km to 50 km. The intercircle polygonal areas (i.e. “rings”) were
250 then employed as blocks to estimate the average Hg concentration. Prior to
251 estimations, blocks were discretised into several small, non-overlapping rectangular
252 cells (100 m x 100 m cell size). Then BK was used to estimate the average Hg
253 concentration for each ring. Finally, 95% confidence intervals (95%CI) were estimated
254 for the block-average Hg concentration based on the estimated BK variance. The
255 kriging neighbourhood for estimating both the block-average Hg concentrations and
256 associated estimation variances was defined as “the soil samples lying within the ring
257 surface, plus the soil samples lying at a distance shorter than 6 km from the ring’s edge
258 in any direction”. The statistical analyses were carried out using the XLSTAT statistical
259 package (Addinsoft Version 2012.2.02), while ISATIS V10.0 and the Geostatistical
260 Analyst extension of ArcMap 10 were used for the geostatistical analyses.

261

262 3. RESULTS AND DISCUSSION

263 3.1 Soil Hg ~~content~~concentrations and temporal changes in sentinel plots.

264 The summary statistics of the Hg ~~content~~concentrations and soil parameters employed
265 to estimate Hg stock are listed in Table 1. No high ~~values were~~concentrations were
266 observed for the Hg concentration in rocky fragments (mean 13.57 $\mu\text{g kg}^{-1}$). Hg
267 ~~content~~concentrations tended to be higher in the soils (mean 64.62 $\mu\text{g kg}^{-1}$) associated
268 with some soil physico-chemical properties, such as organic matter or clay contents
269 (Gruba et al., 2019; Kelepertzis and Argyraki, 2015a; Petrotou et al., 2012; Rodríguez
270 Martín et al., 2009a), but the levels in soil were 5-fold higher than lithogenic content.
271 Mercury contaminated soils constitute complex systems where many interdependent
272 factors, including amount and composition of soil organic matter and clays, oxidized
273 minerals, reduced elements, as well as soil pH and redox conditions affect Hg forms
274 and transformation (O'Connor et al., 2019). Nevertheless, the most important Hg

275 input on the Majorca Island can be associated with human activity. In fact in global
276 terms, the largest Hg contributions to the environment are attributed to human
277 anthropogenic sources (Kelepertzis and Argyraki, 2015b; Mirzaei et al., 2015; Raj and
278 Maiti, 2019; Ravankhah et al., 2017), mainly fossil fuel combustion (Beckers and
279 Rinklebe, 2017; Botsou et al., 2020; Fisher and Nelson, 2020; Pacyna et al., 2006).

280

281 *Table 1: Soil samples and statistical summary of the 2017 descriptive soil parameter sampling.*

282

283 The means soil Hg ~~content~~concentration in Majorcan soil (Tables 1 and 2) is similar to
284 mainland Spanish soil ($60 \mu\text{g kg}^{-1}$) (Rodríguez Martín et al., 2009c), but higher than
285 Europe topsoil Hg ~~content~~concentration ($22 \mu\text{g kg}^{-1}$) (Salminen et al., 2005). Other
286 studies have established an Hg background level of $20 \mu\text{g kg}^{-1}$ (Higuera et al., 2015)
287 and a reference value of $25 \mu\text{g kg}^{-1}$ (Gil et al., 2010) for the Spanish Mediterranean
288 Region. This study observed that 95% soil exceeded these levels. Annual crop soils
289 (mean $70 \mu\text{g kg}^{-1}$) presented maximum Hg ~~values~~concentration ($258 \mu\text{g kg}^{-1}$) (Table 2)
290 in agricultural areas. These high levels can be related to agricultural practices, and also
291 to agrochemicals being constantly incorporated into some annual vegetables crops, and
292 often abusively so (Ramos-Miras et al., 2019; Rodríguez Martín et al., 2013c). However,
293 we were surprised to also find high Hg ~~content~~concentrations in forest soil ($68 \mu\text{g kg}^{-1}$)
294 and holm oaks, or $69 \mu\text{g kg}^{-1}$ in pinewood (Table 2). These concentration levels in
295 forest soil are higher than for other agricultural soils on Majorca, which are associated
296 with atmospheric pollution (Hg air pollution).

297

298 *Table 2: Statistical summary of the Hg concentration in soil according to the land-use classes*
299 *sampling finished in 2017.*

300

301 Based on the Hg ~~content~~concentrations evaluated in the sentinel plots, the Hg
302 concentration in topsoil had increased after 11 years (Table 3). In 2006, the mean Hg
303 ~~content~~concentration in soil was $46.60 \mu\text{g kg}^{-1}$ compared to $62.10 \mu\text{g kg}^{-1}$ recorded in
304 2017 in the same plots. Although this increase exceeds 30%, no clear differences were
305 found to consider it to be statistically significantly according to an ANOVA test. This
306 finding suggests that the observed increase was not homogeneous for the island on the
307 whole, and it is also necessary to consider that the variation in Hg soil
308 ~~content~~concentration among crop types (Table 2) might be more marked than the

309 differences found between years. Therefore, it was necessary to analyse Hg spatial
310 variability in soil to be able to quantify the Hg increase distribution and to locate
311 possible pollution sources on this island.

312

313 *Table 3: Statistical summary of the Hg concentration ($\mu\text{g kg}^{-1}$) in the sentinel plots (28*
314 *samples)*

315

316 **3.2 Spatial variability and assessment of Hg stock on Majorca**

317 Experimental semivariograms are presented in the Supplementary Material (Figure
318 S1), where the exponential model was used to fit the semivariogram. The spatial
319 correlation range was significantly wider for BD (8 km) or stoniness (11 km) than for
320 Hg (4.1 km), which mainly represents the spatial variation corresponding to edaphic
321 influence and soil structure. Evidence for human influence can be associated with soil
322 Hg concentration due to a narrower spatial range than the mineralogical and bedrock
323 influences. Figure 2 shows the kriging map based on the semivariogram. The quality of
324 the prediction maps was examined by the cross-validation technique (Rodríguez
325 Martín et al., 2007). The mean errors and the root-mean-squared standardised errors
326 respectively came close to 0 and 1 (Table S1), which indicate the good accuracy of the
327 kriging maps. The Hg map indicated that some areas on the Majorca Island had high
328 ~~values~~concentration. This was particularly evidenced in the north-eastern part of the
329 island, which can associated with an industrial influence (Rodríguez Martín et al.,
330 2013b) related mainly to atmospheric deposition by the coal-burning power plant (Li et
331 al., 2017; Lv and Liu, 2019; Raj and Maiti, 2019; Rodríguez Martín and Nanos, 2016). In
332 addition, a small area to the east of the island near its capital also presented a high Hg
333 soil concentration. It is known that some urban activities are associated with Hg
334 pollution (Botsou et al., 2020; Trujillo-González et al., 2016; Zhou and Wang, 2019).
335 Higher stoniness percentages were recorded in the north and were associated mainly
336 with forest areas. The BD map showed a more homogeneous distribution with local
337 variation on the shorter scale related to soil compaction (Rodríguez Martín et al., 2016;
338 Trujillo-González et al., 2019).

339

340 *Figure S1: Experimental variogram and spatial models for mercury (Hg) ~~content~~concentration,*
341 *stoniness and bulk density (BD).*

342

343 *Figure 2: Spatial distribution of Hg ~~content~~concentration, stoniness and BD interpolated by*
344 *ordinary kriging.*

345
346 Hg stock (Figure 3) was computed as the product of three variables (Hg concentration,
347 BD and fraction of coarse fragments), which were regionalised by a geostatistical
348 approach. These maps showed Hg accumulation in soil. As we can see, the Hg stock on
349 the island generally increased, mainly in the northeast. In 2006, the highest Hg contents
350 were observed in the vicinity of the Alcudia coal-fired power point (Rodríguez Martín
351 et al., 2013b) where Hg accumulation was 4 g/ha. In 2017, Hg accumulation on the
352 island was more widely dispersed (Figure 3), although greater Hg accumulation was
353 still observed in the same area, and the highest levels had increased from 4.0 to 6.6
354 g/ha during the same 11-year period.

355
356 The Hg stock 2017/Hg stock 2006 ratio was used to identify these areas, which might
357 suggest pollution inputs to evaluate temporal Hg accumulation changes. Hg
358 accumulation in this area was evidenced, where soil Hg stock had tripled in only 11
359 years. ~~The influence and repercussion of coal fired power plants on atmospheric Hg~~
360 ~~emissions are well known (see "Mercury Falling" (Coequyt et al., 1999)). In fact coal~~
361 ~~burning power plants are the main source of Hg pollution (Wang et al., 2010; Yang and~~
362 ~~Wang, 2008). Fossil fuel combustion represents approximately 60% of Hg emissions~~
363 ~~worldwide (Pacyna et al., 2006) and 26% of all Hg emissions (236 tons/year) in~~
364 ~~European electric energy plants (Pacyna et al., 2006). In Spain alone, coal fired electric~~
365 ~~power plants lie behind 47% of all Hg emissions (López Alonso et al., 2003). Some~~
366 ~~studies (Streets et al., 2009) estimate that overall Hg emissions could increase to 96% by~~
367 ~~2050 if new technologies are not set up to control coal fired electric power plants. Hg~~
368 ~~measurements in tree rings also show a continuous increase in atmospheric Hg levels~~
369 ~~between 1975 and the present day (Clackett et al., 2018)). Conversely, research carried~~
370 ~~out by EU GMOS (Global Mercury Observation System) estimate scenarios with an~~
371 ~~85% reduction in Hg emissions by 2035 (Pacyna et al., 2016), which indicates a decrease~~
372 ~~of up to 50% deposition in the Northern Hemisphere compared to 2013. This trend will~~
373 ~~the result of the EU Mercury Strategy and the requirements set by the Minamata~~
374 ~~Convention. It will agree with what the European Commission estimates for the future,~~
375 ~~and with other research works that have indicated lowering Hg accumulation rates in~~
376 ~~the last few decades (Corella et al., 2017) in the Western Mediterranean and fewer~~

~~anthropogenic Hg emissions in the past two decades in the Mediterranean Basin (Cinnirella et al., 2019).~~

Figure 3: Maps of the soil ~~mercury~~Hg stock on the Majorca Island. Values in kg ha⁻¹.

This trend is not evidenced in our case, rather Hg stock in soil considerably increased and does not only presently derive from the power plant, but also from diffuse pollution on the island that is limited mostly to both its geographical area and polluting activity on the island. Tourism pressure, and bigger summer populations (Brtnický et al., 2020) with more than more than 13 million visitors in 2017, are associated with services rendered to tourists, such as electricity, waste management, incinerators, transport, rental vehicles, etc, which also play a key role in the rising Hg levels on the island (Saenz-de-Miera and Rosselló, 2014). Growing populations and cities are undoubtedly associated with more pollution (Kelepertzis and Argyraki, 2015b; Ravankhah et al., 2016; Rodríguez Martín et al., 2015; Trujillo-González et al., 2016). Another area with a bigger Hg stock in soil is in the vicinity of the island's capital (Palma de Majorca) as the contents quantified in 2006 had doubled in 2017. Today Palma de Majorca has a population of 400,000 inhabitants, which is almost half of the whole populating living on the island (907,000 people).

In short, the Hg stock for the Majorca Island on the whole has increased from 432.96 tons in 2006 to 493.18 tons in 2017 (Table 4). This means that more than 60 tons of Hg have accumulated on the island in 11 years. For this same period, the mean Hg deposition figure has been estimated at 33.40 $\mu\text{g m}^{-2} \text{ yr}^{-1}$. This value falls within the wide range of deposition figures described by other studies. For example, Yu et al. (2013) estimated Hg deposition to be 17.4 $\mu\text{g m}^{-2} \text{ yr}^{-1}$ in Adirondack Mountain (New York State, USA) with wide variability (range from 3.7 to 46.0 $\mu\text{g m}^{-2} \text{ yr}^{-1}$). In midcontinental North America (Wisconsin), Swain et al. (1992) quantified Hg deposition to go from ~~1,850 (3.7 0 $\mu\text{g m}^{-2} \text{ yr}^{-1}$)~~ in -1,850 to 12.5 0 $\mu\text{g m}^{-2} \text{ yr}^{-1}$) in recent decades. Wang et al. (2016) assessed global Hg deposition through litterfall, which they estimated was 1,180±710 Mg yr⁻¹ and ranged from 2.7 to 219.9 $\mu\text{g m}^{-2} \text{ yr}^{-1}$) with a mean of 27.439 $\mu\text{g m}^{-2} \text{ yr}^{-1}$, which is a similar estimate to that obtained herein. On Norwegian land based on modelled deposition according to the European Monitoring and Evaluation Programme (EMEP), Braaten et al. (2018) estimated a deposition flux of

411 only 9.5 $\mu\text{g m}^{-2} \text{yr}^{-1}$. However, Steinnes et al. (1991) quantified 35 $\mu\text{g m}^{-2} \text{yr}^{-1}$ near Oslo
412 (Norway). Navratil et al. (2019) evaluated Hg flux trends in the Czech Republic and
413 reported means of 45 and 32 $\mu\text{g m}^{-2} \text{yr}^{-1}$, which lowered in forest soil from 66 $\mu\text{g m}^{-2} \text{yr}^{-1}$
414 in 2003 to 23 $\mu\text{g m}^{-2} \text{yr}^{-1}$ in 2017. ~~This is the completely opposite trend to that observed~~
415 ~~in our study.~~

416

417 *Table 4: Soil mercury stock estimated from the kriging maps for 2006 and 2017.*

418 **3.3 Soil Hg and relations with pollution sources**

419 Soil ~~mercury~~Hg concentration depends primarily on geological parent material (soil-
420 forming factors) (Jimenez Ballesta, 2017; Papastergios et al., 2009; Rodríguez Martín et
421 al., 2009b). The rocky fragments of Hg content can be attributed only to the
422 geochemical processes that correspond to mineralogical structures (Rodríguez Martín
423 et al., 2013a). The Majorca Island is formed mostly by calcareous lithologies that were
424 formed during the Tertiary and do not present high ~~values~~concentration. The
425 concentration ranges in the rocky fragments on the Majorca Island fell between 5.70
426 and 20.50 $\mu\text{g kg}^{-1}$ (mean 13.60 $\mu\text{g kg}^{-1}$) *versus* soil ~~content~~concentrations (mean 64.62 μg
427 kg^{-1}) (Table 1). The topsoil/rock Hg content ratio has been used to evaluate soil Hg
428 enrichment. Soil ~~metal~~-Hg is considered when the metal concentration in soil is 8-fold
429 higher than the lithogenic content (Rodríguez Martín et al., 2013b). Based on the
430 assumption of a distance-dependent effect of coal-fired power plant emissions on Hg
431 soil ~~content~~concentrations, 16 concentric circles (radius of 3 km) centred on the Alcudia
432 power plant were constructed and covered the whole island surface (Figure 4). The
433 mean Hg concentration in soil and the topsoil/rock ratio between two consecutive
434 areas (circles) were computed by BK (Rodriguez Martin et al., 2014).

435

436 *Figure 4: Estimates of soil Hg and the soil/rock ratio computed by concentric circles in block*
437 *kriging and the associated confidence intervals around the Alcudia coal-fired power plant.*

438

439 The soil Hg concentration displayed a decreasing trend according to the distance to the
440 power plant (Figure 4). The highest mean ~~content~~concentration was observed in the
441 second ring (6 km) and the maximum ratio in the third ring (9 km), probably as a result
442 of pipe height preventing fly ash from being deposited on the power plant itself. Soil
443 Hg was 15-fold higher than the lithogenic content near the power plant, which
444 suggests major local enrichment due to emissions. The Hg accumulation in the vicinity

445 of power plants has been reported in many studies (Li et al., 2017; Lv et al., 2019;
446 N6voa-Mu6noz et al., 2008; Rodr6guez Mart6n and Nanos, 2016; Yang and Wang, 2008)
447 and is linked with the carbon Hg content used in power plants (Rodr6guez Martin et
448 al., 2014; Wang et al., 2010). These levels were higher according to the power plant
449 energy capacity (N6voa-Mu6noz et al., 2008), especially in power plants over 1,000 MW
450 (Rodr6guez Mart6n and Nanos, 2016). On Majorca, with a capacity to generate 218 MW,
451 the maximum soil Hg value was 258 $\mu\text{g kg}^{-1}$ (Table 1). On the Spanish mainland, soil
452 ~~content~~concentrations over 1,000 $\mu\text{g kg}^{-1}$ have been reported near similar coal
453 combustion power plants in Castell6n (1650 MW), Abo6o (921 MW) or Soto de Ribera
454 (1481 MW) (Rodr6guez Mart6n and Nanos, 2016). Other studies have also reported soil
455 ~~content~~concentrations above 1,000 $\mu\text{g kg}^{-1}$ in the Baoji Power Plant of China (Yang and
456 Wang, 2008), 1,600 $\mu\text{g kg}^{-1}$ in another Chinese power plant (Yuan et al., 2010) and 2,100
457 $\mu\text{g kg}^{-1}$ in the Serbian Nikola Tesla power plant (Dragovi6 et al., 2013).

458

459 To summarise, coal-burning power plants are a relevant source of Hg emissions
460 (Coequyt et al., 1999; Furl and Meredith, 2011; Wang et al., 2010; Yang and Wang, 2008)
461 that often cause Hg enrichment in soils associated with atmospheric deposition (Li et
462 al., 2017; Lv et al., 2019; Rodr6guez Martin et al., 2018). Hg volatilised during coal
463 combustion comes into contact with fly ash which, given its large specific area, is
464 finally enriched before escaping stack. This ash is deposited near power plants (Keeler
465 et al., 2006; Li et al., 2017; Rodriguez Martin et al., 2014). According to Figure 4, the
466 effect of the Alcudia coal-fired power plant on soil is limited to distances < 18 km,
467 which is a similar range to that observed in other studies (Li et al., 2017; Nanos et al.,
468 2015; Rodr6guez Mart6n and Nanos, 2016). In this way, Hg ~~content~~concentrations in soil
469 increase compared to the contribution from ~~-~~weathering rocks. The present study
470 shows that the Alcudia power plant is the main local pollution source on the Majorca
471 Island. Its local influence on Hg soil ~~content~~concentration rapidly decreases with
472 distance, but diffuse pollution can affect the whole island by increasing Hg
473 accumulation in soil through atmospheric deposition.

474

475 **4 CONCLUSIONS**

476 Spatial patterns provided valuable information to quantify and evaluate Hg stock
477 trends. In line with the results of this study, we conclude that soil Hg levels have
478 substantially increased on the Majorca Island due to human activities. Interpolated

479 maps show that Hg ~~content~~concentration in topsoil has doubled in the vicinity of the
480 Alcudia coal-fired power plant in 11 years. Although the degree of pollution is high,
481 spatial patterns revealed that the most widely emitted Hg is deposited at distances less
482 than 18 km. However, the effects of the Hg emissions from the coal-burning power
483 plant are stronger every year and Hg deposition can be hazardous in the future if a
484 rising trend persists.

485

486 A significant influence of tourism on the island's Hg contamination has been proved.
487 Population growth during holiday seasons increases atmospheric deposition by
488 rendering necessary services to tourists and related activities. In short, more than 60
489 tons of Hg have accumulated on this island in 11 years. Soil contamination on the
490 Majorca Island is expected to grow, which will have a negative impact on local
491 ecosystems. More environmental awareness is necessary in both the energy and
492 tourism sectors. According to the UN Sustainable Development Goals (SDG) and the
493 2020 Environmental Action Programme motto, "Living well, within the limits of our
494 planets" in the EU policy action, we hope that measures will be taken to conserve and
495 protect this island from increased pollution, which will involve taking actions to
496 reduce both the number of tourists and atmospheric deposition from the coal-fired
497 power plant. Presently certain technology, such as activated carbon injection, can
498 reduce emissions by 90%.

499

500 **5- ACKNOWLEDGEMENTS:**

501 We greatly appreciate the financial assistance provided by Spanish Ministry (Project
502 CGL2013-43675-P) and CAM (Project AGRISOST-CM S2018/BAA-4330).

503

504 **6- REFERENCES**

- 505 Beckers, F., Rinklebe, J., 2017. Cycling of mercury in the environment: Sources, fate,
506 and human health implications: A review. *Critical Reviews in Environmental*
507 *Science and Technology* 47, 693-794.
- 508 Black, G., Hartge, K., 1986. Bulk density. *Methods of soil analysis*. Part 1, 347-380.
- 509 Botsou, F., Moutafis, I., Dalaina, S., Kelepertzis, E., 2020. Settled bus dust as a proxy of
510 traffic-related emissions and health implications of exposures to potentially harmful
511 elements. *Atmospheric Pollution Research* 11, 1776-1784.
- 512 Braaten, H.F.V., Gundersen, C.B., Sample, J.E., Selvik, J.R., de Wit, H., 2018.
513 Atmospheric deposition and lateral transport of mercury in Norwegian drainage
514 basins: A mercury budget for Norway. NIVA-rapport.
- 515 Brtnický, M., Pecina, V., Galiová, M.V., Prokeš, L., Zvěřina, O., Juříčka, D., Klimánek,
516 M., Kynický, J., 2020. The impact of tourism on extremely visited volcanic island:

517 Link between environmental pollution and transportation modes. *Chemosphere*
518 249, 126118.

519 Cinnirella, S., Bruno, D.E., Pirrone, N., Horvat, M., Živković, I., Evers, D., Johnson, S.,
520 Sunderland, E., 2019. Mercury concentrations in biota in the Mediterranean Sea, a
521 compilation of 40 years of surveys. *Scientific data* 6, 1-11.

522 Clackett, S.P., Porter, T.J., Lehnherr, I., 2018. 400-year record of atmospheric mercury
523 from tree-rings in northwestern Canada. *Environmental Science & Technology* 52,
524 9625-9633.

525 Coequyt, J., Group, E.W., Council, N.R.D., Network, C.A., 1999. Mercury Falling: An
526 analysis of mercury pollution from coal-burning power plants. Environmental
527 Working Group.

528 Corella, J.P., Valero-Garcés, B.L., Wang, F., Martínez-Cortizas, A., Cuevas, C., Saiz-
529 Lopez, A., 2017. 700 years reconstruction of mercury and lead atmospheric
530 deposition in the Pyrenees (NE Spain). *Atmospheric Environment* 155, 97-107.

531 Chilés, J.P., Delfiner, P., 1999. *Geostatistics: Modeling Spatial Uncertainty*. John Wiley
532 & Sons, Inc, New York.

533 Dragović, S., Čujić, M., Slavković-Beškoski, L., Gajić, B., Bajat, B., Kilibarda, M., Onjia,
534 A., 2013. Trace element distribution in surface soils from a coal burning power
535 production area: A case study from the largest power plant site in Serbia. *CATENA*
536 104, 288-296.

537 [During, A., Rinklebe, J., Boehme, F., Wennrich, R., Staerk, H.-J., Mothes, S., Du Laing,](#)
538 [G., Schulz, E., Neue, H.-U., 2009. Mercury volatilization from three floodplain soils](#)
539 [at the Central Elbe River, Germany. *Soil and Sediment Contamination* 18, 429-444](#)

540 Fisher, J.A., Nelson, P.F., 2020. Atmospheric mercury in Australia: Recent findings and
541 future research needs. *Elementa: Science of the Anthropocene* 8.

542 Furl, C., Meredith, C., 2011. Mercury Accumulation in Sediment Cores from Three
543 Washington State Lakes: Evidence for Local Deposition from a Coal-Fired Power
544 Plant. *Archives of Environmental Contamination and Toxicology* 60, 26-33.

545 Gil, C., Ramos-Miras, J., Roca-Pérez, L., Boluda, R., 2010. Determination and
546 assessment of mercury content in calcareous soils. *Chemosphere* 78, 409-415.

547 Gruba, P., Socha, J., Pietrzykowski, M., Pasichnyk, D., 2019. Tree species affects the
548 concentration of total mercury (Hg) in forest soils: Evidence from a forest soil
549 inventory in Poland. *Science of The Total Environment* 647, 141-148.

550 Gutiérrez, C., Fernández, C., Escuer, M., Campos-Herrera, R., Beltrán Rodríguez, M.E.,
551 Carbonell, G., Rodríguez Martín, J.A., 2016. Effect of soil properties, heavy metals
552 and emerging contaminants in the soil nematodes diversity. *Environmental*
553 *Pollution* 213, 184-194.

554 Higuera, P., Fernández-Martínez, R., Esbrí, J., Rucandio, I., Loredó, J., Ordóñez, A.,
555 Álvarez, R., 2015. Mercury Soil Pollution in Spain: A Review, in: Jiménez, E.,
556 Cabañas, B., Lefebvre, G. (Eds.), *Environment, Energy and Climate Change I*.
557 Springer International Publishing, pp. 135-158.

558 Isatis, 2015. *Isatis software manual*. Geovariances & Ecole des Mines de Paris, Paris.

559 Jimenez Ballesta, R., 2017. *Introducción a la contaminación de suelos*. Mundi-Prensa
560 Libros.

561 Keeler, G.J., Landis, M.S., Norris, G.A., Christianson, E.M., Dvonch, J.T., 2006. Sources
562 of Mercury Wet Deposition in Eastern Ohio, USA. *Environmental Science &*
563 *Technology* 40, 5874-5881.

564 Kelepertzis, E., Argyraki, A., 2015a. Geochemical associations for evaluating the
565 availability of potentially harmful elements in urban soils: Lessons learnt from
566 Athens, Greece. *Applied Geochemistry* 59, 63-73.

- 567 Kelepertzis, E., Argyraki, A., 2015b. Mercury in the Urban Topsoil of Athens, Greece.
568 Sustainability 7, 4049-4062.
- 569 Li, R., Wu, H., Ding, J., Fu, W., Gan, L., Li, Y., 2017. Mercury pollution in vegetables,
570 grains and soils from areas surrounding coal-fired power plants. Scientific Reports
571 7, 46545.
- 572 López Alonso, M., Benedito, J.L., Miranda, M., Fernández, J.A., Castillo, C., Hernández,
573 J., Shore, R.F., 2003. Large-scale spatial variation in mercury concentrations in cattle
574 in NW Spain. Environmental Pollution 125, 173-181.
- 575 Lv, J., Liu, Y., 2019. An integrated approach to identify quantitative sources and
576 hazardous areas of heavy metals in soils. Science of The Total Environment 646, 19-
577 28.
- 578 Lv, J., Xia, Q., Yan, T., Zhang, M., Wang, Z., Zhu, L., 2019. Identifying the sources,
579 spatial distributions, and pollution status of heavy metals in soils from the southern
580 coast of Laizhou Bay, eastern China. Human and Ecological Risk Assessment: An
581 International Journal 25, 1953-1967.
- 582 Mikayilov, J.I., Mukhtarov, S., Mammadov, J., Azizov, M., 2019. Re-evaluating the
583 environmental impacts of tourism: does EKC exist? Environmental Science and
584 Pollution Research 26, 19389-19402.
- 585 Mirzaei, R., Teymourzade, S., Sakizadeh, M., Ghorbani, H., 2015. Comparative study of
586 heavy metals concentration in topsoil of urban green space and agricultural land
587 uses. Environmental Monitoring and Assessment 187, 741.
- 588 Nanos, N., Grigoratos, T., Rodríguez Martín, J., Samara, C., 2015. Scale-dependent
589 correlations between soil heavy metals and As around four coal-fired power plants
590 of northern Greece. Stochastic Environmental Research and Risk Assessment 29,
591 1531-1543.
- 592 Navrátil, T., Nováková, T., Roll, M., Shanley, J.B., Kopáček, J., Rohovec, J., Kaňa, J.,
593 Cudlín, P., 2019. Decreasing litterfall mercury deposition in central European
594 coniferous forests and effects of bark beetle infestation. Science of The Total
595 Environment 682, 213-225.
- 596 Nóvoa-Muñoz, J.C., Pontevedra-Pombal, X., Martínez-Cortizas, A., García-Rodeja
597 Gayoso, E., 2008. Mercury accumulation in upland acid forest ecosystems nearby a
598 coal-fired power-plant in Southwest Europe (Galicia, NW Spain). Science of The
599 Total Environment 394, 303-312.
- 600 [O'Connor, D., Hou, D., Ok, Y.S., Mulder, J., Duan, L., Wu, Q., Wang, S., Tack, F.M.,](#)
601 [Rinklebe, J., 2019. Mercury speciation, transformation, and transportation in soils,](#)
602 [atmospheric flux, and implications for risk management: A critical review.](#)
603 [Environment International 126, 747-761.](#)
- 604 Odumo, B., Carbonell, G., Angeyo, H., Patel, J., Torrijos, M., Rodríguez Martín, J., 2014.
605 Impact of gold mining associated with mercury contamination in soil, biota
606 sediments and tailings in Kenya. Environmental Science and Pollution Research 21,
607 12426-12435.
- 608 Pacyna, E.G., Pacyna, J.M., Fudala, J., Strzelecka-Jastrzab, E., Hlawiczka, S., Panasiuk,
609 D., 2006. Mercury emissions to the atmosphere from anthropogenic sources in
610 Europe in 2000 and their scenarios until 2020. Science of The Total Environment 370,
611 147-156.
- 612 Pacyna, J.M., Travnikov, O., Simone, F.d., Hedgecock, I.M., Sundseth, K., Pacyna, E.G.,
613 Steenhuisen, F., Pirrone, N., Munthe, J., Kindbom, K., 2016. Current and future
614 levels of mercury atmospheric pollution on a global scale.
- 615 Papastergios, G., Fernández-Turiel, J.-L., Georgakopoulos, A., Gimeno, D., 2009.
616 Natural and anthropogenic effects on the sediment geochemistry of Nestos River,
617 northern Greece. Environmental Geology 58, 1361-1370.

618 Petrotou, A., Skordas, K., Papastergios, G., Filippidis, A., 2012. Factors affecting the
619 distribution of potentially toxic elements in surface soils around an industrialized
620 area of northwestern Greece. *Environmental Earth Sciences* 65, 823-833.

621 Raj, D., Maiti, S.K., 2019. Sources, toxicity, and remediation of mercury: an essence
622 review. *Environmental Monitoring and Assessment* 191, 566.

623 Ramos-Miras, J.J., Gil, C., Rodríguez Martín, J.A., Bech, J., Boluda, R., 2019. Ecological
624 risk assessment of mercury and chromium in greenhouse soils. *Environmental*
625 *Geochemistry and Health*.

626 Ravankhah, N., Mirzaei, R., Masoum, S., 2016. Spatial eco-risk assessment of heavy
627 metals in the surface soils of industrial city of Aran-o-Bidgol, Iran. *Bulletin of*
628 *Environmental Contamination and Toxicology* 96, 516-523.

629 Ravankhah, N., Mirzaei, R., Masoum, S., 2017. Determination of heavy metals in
630 surface soils around the brick kilns in an arid region, Iran. *Journal of Geochemical*
631 *Exploration* 176, 91-99.

632 [Rinklebe, J., Doring, A., Overesch, M., Du Laing, G., Wennrich, R., Stärk, H.-J., Mothes,](#)
633 [S., 2010. Dynamics of mercury fluxes and their controlling factors in large Hg-](#)
634 [polluted floodplain areas. *Environmental Pollution* 158, 308-318.](#)

635 Rodríguez Martín, J., Carbonell Martín, G., López Arias, M., Grau Corbí, J., 2009a.
636 Mercury content in topsoils, and geostatistical methods to identify anthropogenic
637 input in the Ebro basin (Spain). *Spanish Journal of Agricultural Research* 7, 107-118.

638 Rodríguez Martín, J., Nanos, N., Grigoratos, T., Carbonell, G., Samara, C., 2014. Local
639 deposition of mercury in topsoils around coal-fired power plants: is it always true?
640 *Environmental Science and Pollution Research* 21, 10205-10214.

641 Rodríguez Martín, J., Nanos, N., Miranda, J., Carbonell, G., Gil, L., 2013a. Volcanic
642 mercury in *Pinus canariensis*. *Naturwissenschaften* 100, 739-747.

643 Rodríguez Martín, J., Vázquez de la Cueva, A., Grau Corbí, J., López Arias, M., 2007.
644 Factors Controlling the Spatial Variability of Copper in Topsoils of the Northeastern
645 Region of the Iberian Peninsula, Spain. *Water, Air, & Soil Pollution* 186, 311-321.

646 Rodríguez Martín, J., Vazquez de la Cueva, A., Grau Corbí, J., Martínez Alonso, C.,
647 López Arias, M., 2009b. Factors controlling the spatial variability of mercury
648 distribution in Spanish topsoil. *Soil & Sediment Contamination* 18, 30-42.

649 Rodríguez Martín, J.A., Álvaro-Fuentes, J., Gonzalo, J., Gil, C., Ramos-Miras, J.J., Grau
650 Corbí, J.M., Boluda, R., 2016. Assessment of the soil organic carbon stock in Spain.
651 *Geoderma* 264, Part A, 117-125.

652 Rodríguez Martín, J.A., Carbonell, G., Nanos, N., Gutiérrez, C., 2013b. Source
653 Identification of Soil Mercury in the Spanish Islands. *Archives of Environmental*
654 *Contamination and Toxicology* 64, 171-179.

655 Rodríguez Martín, J.A., De Arana, C., Ramos-Miras, J.J., Gil, C., Boluda, R., 2015.
656 Impact of 70 years urban growth associated with heavy metal pollution.
657 *Environmental Pollution* 196, 156-163.

658 Rodríguez Martín, J.A., Gutiérrez, C., Torrijos, M., Nanos, N., 2018. Wood and bark of
659 *Pinus halepensis* as archives of heavy metal pollution in the Mediterranean Region.
660 *Environmental Pollution* 239, 438-447.

661 Rodríguez Martín, J.A., López Arias, M., Grau Corbí, J.M., 2009c. Metales pesados,
662 materia organica y otros parametros de los suelos agricolas y de pastos de España.
663 Ministerio de medio ambiente y medio rural y marino / Instituto Nacional de
664 Investigación y Tecnología Agraria y Alimentaria. , Madrid.

665 Rodríguez Martín, J.A., Nanos, N., 2016. Soil as an archive of coal-fired power plant
666 mercury deposition. *Journal of Hazardous Materials* 308, 131-138.

667 Rodríguez Martín, J.A., Ramos-Miras, J.J., Boluda, R., Gil, C., 2013c. Spatial relations of
668 heavy metals in arable and greenhouse soils of a Mediterranean environment region
669 (Spain). *Geoderma* 200–201, 180-188.

670 Saenz-de-Miera, O., Rosselló, J., 2014. Modeling tourism impacts on air pollution: The
671 case study of PM10 in Mallorca. *Tourism Management* 40, 273-281.

672 Salminen, R., Plant, J., Reeder, S., 2005. Geochemical atlas of Europe. Part 1,
673 Background information, methodology and maps. Geological survey of Finland.

674 Steinnes, E., Berg, T., Sjøbakk, T., 2003. Temporal and spatial trends in Hg deposition
675 monitored by moss analysis. *Science of The Total Environment* 304, 215-219.

676 Streets, D.G., Zhang, Q., Wu, Y., 2009. Projections of Global Mercury Emissions in 2050.
677 *Environmental Science & Technology* 43, 2983-2988.

678 Swain, E.B., Engstrom, D.R., Brigham, M.E., Henning, T.A., Brezonik, P.L., 1992.
679 Increasing rates of atmospheric mercury deposition in midcontinental North
680 America. *Science* 257, 784-787.

681 Trujillo-González, J.M., Torres-Mora, M.A., Jiménez-Ballesta, R., Zhang, J., 2019. Land-
682 use-dependent spatial variation and exposure risk of heavy metals in road-
683 deposited sediment in Villavicencio, Colombia. *Environmental Geochemistry and*
684 *Health* 41, 667-679.

685 Trujillo-González, J.M., Torres-Mora, M.A., Keesstra, S., Brevik, E.C., Jiménez-Ballesta,
686 R., 2016. Heavy metal accumulation related to population density in road dust
687 samples taken from urban sites under different land uses. *Science of The Total*
688 *Environment* 553, 636-642.

689 Wang, L., Hou, D., Cao, Y., Ok, Y.S., Tack, F.M.G., Rinklebe, J., O'Connor, D., 2020.
690 Remediation of mercury contaminated soil, water, and air: A review of emerging
691 materials and innovative technologies. *Environment International* 134, 105281.

692 Wang, S., Zhang, L., Li, G., Wu, Y., Hao, J., Pirrone, N., Sprovieri, F., Ancora, M., 2010.
693 Mercury emission and speciation of coal-fired power plants in China. *Atmospheric*
694 *Chemistry and Physics* 10, 1183-1192.

695 Wang, X., Bao, Z., Lin, C.-J., Yuan, W., Feng, X., 2016. Assessment of global mercury
696 deposition through litterfall. *Environmental Science & Technology* 50, 8548-8557.

697 Wu, Q., Wang, S., Li, G., Liang, S., Lin, C.-J., Wang, Y., Cai, S., Liu, K., Hao, J., 2016.
698 Temporal trend and spatial distribution of speciated atmospheric mercury
699 emissions in China during 1978–2014. *Environmental Science & Technology* 50,
700 13428-13435.

701 Yang, X., Wang, L., 2008. Spatial analysis and hazard assessment of mercury in soil
702 around the coal-fired power plant: a case study from the city of Baoji, China.
703 *Environmental Geology* 53, 1381-1388.

704 Yu, X., Driscoll, C.T., Huang, J., Holsen, T.M., Blackwell, B.D., 2013. Modeling and
705 mapping of atmospheric mercury deposition in Adirondack Park, New York. *PLoS*
706 *ONE* 8.

707 Yuan, C.-G., Wang, T.-F., Song, Y.-F., Chang, A.-L., 2010. Total mercury and
708 sequentially extracted mercury fractions in soil near a coal-fired power plant.
709 *Fresenius Environmental Bulletin* 19, 2857-2863.

710 Zhang, L., Wong, M., 2007. Environmental mercury contamination in China: sources
711 and impacts. *Environment International* 33, 108-121.

712 Zhou, X.-Y., Wang, X.-R., 2019. Impact of industrial activities on heavy metal
713 contamination in soils in three major urban agglomerations of China. *Journal of*
714 *Cleaner production* 230, 1-10.

715